HHS Public Access

Author manuscript

Cell Rep. Author manuscript; available in PMC 2017 December 01.

Published in final edited form as:

Cell Rep. 2016 September 06; 16(10): 2666–2685. doi:10.1016/j.celrep.2016.08.004.

Tcf4 Regulates Synaptic Plasticity, DNA Methylation, and Memory Function

Andrew J. Kennedy[1,2], **Elizabeth J. Rahn**[1], **Brynna S. Paulukaitis**[1,5], **Katherine E. Savell**[1], **Holly B. Kordasiewicz**[3], **Jing Wang**[1], **John W. Lewis**[1], **Jessica Posey**[1], **Sarah K. Strange**[1], **Mikael C. Guzman-Karlsson**[1], **Scott E. Phillips**[1], **Kyle Decker**[1], **S. Timothy Motley**[4], **Eric E. Swayze**[3], **David J. Ecker**[4], **Todd P. Michael**[4], **Jeremy J. Day**[1], and **J. David Sweatt**[1,5,6,*]

[1]Department of Neurobiology and Evelyn F. McKnight Brain Institute, University of Alabama at Birmingham, Birmingham, AL 35294, USA

[2]Department of Chemistry, Bates College, Lewiston, ME 04240, USA

[3]Ionis Pharmaceuticals, Carlsbad, CA 92010, USA

[4]Ibis Biosciences, Carlsbad, CA 92008, USA

[5]Department of Pharmacology, Vanderbilt University, Nashville, TN 37232, USA

SUMMARY

Human haploinsufficiency of the transcription factor *Tcf4* leads to a rare autism spectrum disorder called Pitt-Hopkins syndrome (PTHS), which is associated with severe language impairment and development delay. Here, we demonstrate that *Tcf4* haploinsufficient mice have deficits in social interaction, ultrasonic vocalization, prepulse inhibition, and spatial and associative learning and memory. Despite learning deficits, *Tcf4*(+/−) mice have enhanced long-term potentiation in the CA1 area of the hippocampus. In translationally oriented studies, we found that small-molecule HDAC inhibitors normalized hippocampal LTP and memory recall. A comprehensive set of next-generation sequencing experiments of hippocampal mRNA and methylated DNA isolated from *Tcf4*-deficient and WT mice before or shortly after experiential learning, with or without administration of vorinostat, identified “memory-associated” genes modulated by HDAC inhibition and dysregulated by *Tcf4* haploinsufficiency. Finally, we observed that *Hdac2* isoform-selective knockdown was sufficient to rescue memory deficits in *Tcf4*(+/−) mice.

*Correspondence: david.sweatt@vanderbilt.edu.
[6]Lead Contact

SUPPLEMENTAL INFORMATION

Supplemental Information includes Supplemental Experimental Procedures, eight figures, and seven tables and can be found with this article online at http://dx.doi.org/10.1016/j.celrep.2016.08.004.

AUTHOR CONTRIBUTIONS

A.J.K. and J.D.S. designed, performed, and analyzed all experiments except the following: A.J.K., M.C.G.-K., and J.J.D. performed bioinformatic analyses. E.J.R. performed motor control assessments. B.S.P. and S.K.S. performed expression analysis. J.W.L. aided in genotyping and colony maintenance. J.P. and S.E.P. aided with ICV injections. J.W. performed electrophysiology. K.D. aided with animal behavior. K.E.S. and J.J.D. performed the bisulfite sequencing. M.C.G.-K. performed the primary neuronal culture experiments. H.B.K. and E.E.S. designed and screened the *HDAC2* ASO library. S.T.M., D.J.E., J.J.D., and T.P.M. aided with experimental design and analysis.

CONFLICTS OF INTEREST

S.T.M., D.J.E., and T.P.M. are Abbott employees. H.B.K. and E.E.S. are employees of Ionis Pharmaceuticals.

Graphical abstract

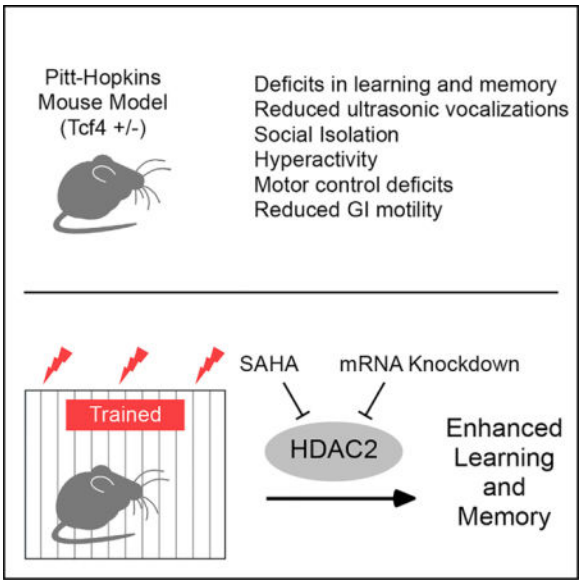

INTRODUCTION

Transcription factor 4 (*Tcf4* aka E2-2, ITF-2, and SEF-2) is necessary for neurodevelopment and plays an important role in cognition, being associated with both schizophrenia and autism-spectrum intellectual disability (ID) (Forrest et al., 2014; Sweatt, 2013). *Tcf4* also has an intimate relationship with verbal memory and language development. A series of intronic SNPs in the *Tcf4* locus have been identified by genome-wide association studies as highly correlative with schizophrenia. The *Tcf4* rs9960767 SNP disrupts sensory-motor gating in both schizophrenia-spectrum and healthy volunteers alike and enhances verbal memory in schizophrenic patients that carry the rs9960767 risk allele without measurably affecting attention and executive function (Lennertz et al., 2011; Quednow et al., 2011). Loss-of-function mutations in *Tcf4* lead to the near-complete lack of language acquisition and cause the rare ID known as Pitt-Hopkins syndrome (PTHS). Altogether, it is likely that *Tcf4* regulation of CNS gene transcription is an underlying process in language comprehension, production, and recall.

As a member of the basic helix-loop-helix (bHLH) transcription factor structural family known as E proteins, *Tcf4* recognizes the Ephrussi box (E-Box) DNA element (5′-CANNTG-3′). *Tcf4* affects chromatin remolding and transcription through the recruitment of histone acetyltransferases (HATs) such as p300 (Bayly et al., 2004; Massari et al., 1999; Zhang et al., 2004). *Tcf4* binds the pseudo-palindromic E-Box via homo-dimerization or hetero-dimerization with other bHLH transcription factors. PTHS mutations occur almost exclusively in the bHLH domain of *Tcf4*, mutating basic residues that are necessary for DNA association or that disrupt bHLH dimerization (Sepp et al., 2012) and leading to a loss-of-function and *Tcf4* haploinsufficiency. PTHS [*Tcf4*(+/−)] is characterized by ID, pronounced developmental delay, lack of motor coordination, epilepsy, breathing abnormalities, autistic behaviors, and language impairment, in most cases with little to no

language usage throughout the lifespan (de Pontual et al., 2009; Ghosh et al., 2012; Peippo and Ignatius, 2012). Few studies have addressed treatment, and currently there is no effective therapy for the cognitive deficits of PTHS (Blake et al., 2010; Zweier et al., 2008). Valproate has been prescribed to treat the epileptic seizures often incurred by PTHS, and one report noted improvement of breathing abnormalities after valproate (Maini et al., 2012). This is intriguing, because one of valproate's mechanisms of action is HDAC inhibition, and a major role of *Tcf4* appears to be the regulation of histone acetylation state. As an aside, it is important to distinguish *Tcf4* from the immune cell regulator T cell factor 4 (*Tcf7l2*), member of the TCF/LEF family of transcription factors and commonly, and erroneously, referred to as TCF4 in the literature.

Two genes, *Nrxn1* and *Cntnap2*, both in the neurexin family of cell adhesion molecules, are believed to be downstream targets of *Tcf4*, because the knockout of either leads to a phenotype similar to that of PTHS, known as PTHS-like 1 and 2, respectively. However, little else is known about the transcriptional consequences of *Tcf4* haploinsufficiency in the brain or whether *Tcf4* affects synaptic plasticity and hippocampal function associated with learning and memory. To begin investigating *Tcf4* function in cognition, we first characterized a PTHS mouse model for deficits in memory and dysregulated synaptic plasticity in the hippocampus. Thus, we would have a model to test the transcriptional and epigenetic mechanisms dysregulated by *Tcf4* haploinsufficiency and test the hypothesis that HDAC inhibition is a therapeutic route to treat the cognitive deficits associated with PTHS.

RESULTS

Tcf4(+/−) Mouse Models PTHS

To further understanding of the neurobiological consequences of *Tcf4* haploinsufficiency, we assessed a *Tcf4*(+/−) mouse with a deletion of the exons that code for the bHLH domain as a potential model for PTHS (Grubišić et al., 2015; Zhuang et al., 1996). Approximately seven out of ten PTHS cases are caused by SNPs that generate a premature stop codon or a point mutation in the bHLH domain of Tcf4 protein (Sepp et al., 2012), disrupting either transcription factor dimerization or mutating one of the basic residues required for DNA backbone association (Figure 1A). The concentration of PTHS SNPs in the bHLH motif highlights a more specific molecular feature of PTHS, namely, the loss of Tcf4 protein and DNA association, and distinguishes them from other SNPs elsewhere in the *Tcf4* locus that are strongly associated with schizophrenia. The *Tcf4*(+/−) mouse should therefore be a functional model of PTHS rather than schizophrenia per se, because the coding region for the bHLH domain has been deleted.

A behavioral battery was undertaken to determine whether *Tcf4*(+/−) mice have motor control differences, have learning and memory deficits, or display behavior akin to other rodent models of autism spectrum disorders (ASDs). *Tcf4*(+/−) mice show no apparent increase in anxiety, as assessed by an open field task and the elevated plus maze; however, both paradigms detect a significant increase in activity (Figures 1B–1F). When placed in an open field, *Tcf4*(+/−) mice have no significant difference in ambulation during the first minute block of the 30 min trial. However, as the experiment continues, they have consistently higher activity without affecting the overall time spent in the center of the field.

Hyperactivity was also detected in the elevated plus maze, where *Tcf4*(+/−) mice show an increase in overall arm entrances without spending a significantly increased amount of time in the open arms.

PTHS patients have marked problems with motor coordination and balance, and we hypothesized that *Tcf4*(+/−) mice would exhibit similar deficits in balance and motor control or learning. We found that *Tcf4*(+/−) mice had asymmetry in their motor control and an imbalance that favors their left side. Dynamic weight bearing, which is the measure of how much force is placed on each paw at rest, was used to assess balance, and *Tcf4*(+/−) mice placed significantly more weight on their front left paw than their right (Figure 1G). Similarly, *Tcf4*(+/−) mice favored their front left paw while ambulating across a catwalk. Figure 1H contains representative images of front-paw pressures collected during the catwalk assessment, where the heatmap indicates the pressure gradient across the paw. In both experiments, *Tcf4*(+/−) mice significantly underuse their front right paw relative to their left and relative to the front right paws of wild-type (WT) controls (Figure S1). In addition, *Tcf4*(+/−) mice show significantly weaker hindlimb, but not forelimb, grip strength (Figure S2).

To determine whether there were deficits with coordination and motor learning in performing more challenging tasks, *Tcf4*(+/−) mice were also made to walk across a horizontal ladder and balance on a rotating rod (Figure S2). The horizontal ladder task assesses the time required for the animal to transit the ladder and measures the number of errors the animals commits in the process in the form of missing a rung of the ladder. The rotating rod task measures coordination, as well as motor learning and memory, because the task is repeated over the course of several trials and days. The *Tcf4*(+/−) mice showed no significant difference in the performance of either test, suggesting that while there are balance and coordination asymmetries, those deficits are not sufficient to impair performance on activity-dependent tasks.

PTHS is an ASD with the predominant phenotype of severe language impairment, and mouse models of ASDs have shown deficits in social interactions (Roullet and Crawley, 2011). To determine whether *Tcf4*(+/−) mice display social aversion or indifference, test mice were submitted to a three-chamber experiment, wherein the distal chambers contained either an empty cylindrical cage or a cylindrical cage holding a novel mouse of equivalent age, gender, and strain. Neurotypical mouse behavior favors social interaction over isolation, and WT controls held in isolation for 10 days spend significantly more time in the chamber holding the novel mouse than that with the empty cage (Crawley, 2004); however, *Tcf4*(+/−) mice preferred social isolation over interaction (Figure 1I). In addition, ASD mouse models often display repetitive behaviors, including increased grooming (Crawley, 2012), and *Tcf4*(+/−) mice groom themselves significantly more than WT mice (Figure S2). *Tcf4*(+/−) mice are hyperreflexive and have significant deficits in prepulse inhibition, highlighting the connection between *Tcf4* and schizophrenia and autism, because a feature of these disorders is dysregulation of sensorimotor gating (Figures 1J and 1K).

Loss-of-function mutations in other transcription factors important in language development, most notably *FOXP2*, causes a reduction in ultrasonic vocalizations (USVs) for young pups

when they are removed from the nest (Fujita et al., 2008; Shu et al., 2005). When pups (post-natal day 3, or P3) are removed from the nest, they elicit USVs as a mechanism meant to notify their mother, a process believed to have cognitive similarities to those processes that underlie language in humans. *Tcf4*(+/−) pups (P3) have significantly reduced USV occurrence, which remains low until the phenotype converges with normal behavior or WT controls around P7 (Figures 1L and 1M; Figure S3). *Tcf4*(+/−) pups (P3) also have significantly weaker calls when measuring the maximum pressure (in decibels) between 20 and 100 kHz during the 5 min test window (Figure 1N). Like spontaneous USVs, ultrasonic distress calls are similarly less frequent and at lower volumes at 3 days of age for *Tcf4*(+/−) pups (Figure S4).

To determine whether the *Tcf4*(+/−) mouse model shows the cognitive deficits associated with PTHS, we assessed their spatial and associative learning and memory using behavioral paradigms. The Morris water maze (MWM) is a classic hippocampus-dependent task that is used to evaluate spatial learning and memory. The MWM consists of teaching a rodent to use distal visual cues to locate a hidden platform just beneath the surface of the water in a circular pool. At first, the mouse finds the platform by chance, but after several subsequent trials, the mouse learns to use the visual cues present to locate the platform from several starting points at the pool's edge. After training, 24 hr memory was tested by removing the platform from the pool, measuring the amount of time spent in the quadrant in which the platform was located, and counting the number of occurrences wherein the mouse crosses over the platform zone during a 60 s trial. *Tcf4*(+/−) mice failed to show selectivity for the target quadrant, spending significantly less time there than did the WT mice and crossing the platform zone significantly fewer times (Figures 2A–2C), despite having unimpaired visible-platform learning and similar average swim speed (Figure S2). Similarly, *Tcf4*(+/−) mice have a significant deficit in 24 hr object location memory (OLM), another hippocampus-dependent spatial memory task (Figure 2D). Mice were given 10 min to interact with two equivalent 50 ml beakers. Memory was assessed by moving one of the beakers to a novel location of the test chamber and measuring the amount of time the test mouse expressed interest in that beaker compared with the beaker in the familiar location over a 5 min test. Altogether, the MWM and OLM tasks elucidate a profound impairment of spatial learning and memory in *Tcf4*(+/−) mice.

We also performed tests of contextual and trace threat recognition training, known as classical fear conditioning, to assess hippocampus-dependent associative learning and memory. In threat recognition training, a conditioned stimulus (CS), a tone and/or context, is paired with an unconditioned stimulus (US), a mild foot shock. Learning and memory is then assessed by measuring the freeze response caused by re-exposure to the training context or to the cue presented in a novel context. For our experiments, a "trace" protocol was used to pair three white noise tones (CS) with a foot shock (US) presented 15 s after the end of the CS (Figure 2E), and then contextual and cued tests were performed 24 hr after training (Figures 2F and 2G). The contextual and trace cued tests are hippocampus-dependent associations, and *Tcf4*(+/−) mice showed significantly reduced freezing in both.

Given the observation that *Tcf4*(+/−) mice have deficits in hippocampus-dependent learning and memory paradigms, we expected that long-term potentiation (LTP) at Schaffer

collaterals between CA3 and CA1 in the hippocampus would be attenuated, because LTP in the hippocampus is known to subserve learning in these tasks. Surprisingly, we found that *Tcf4*(+/−) mice have enhanced Schaffer collateral LTP when activated with theta burst stimulation (Figure 2H). Enhanced LTP coupled with learning and memory deficits is uncommon but not unprecedented for models of ID (Gu et al., 2002).

Altogether, these baseline assessments of behavior and electrophysiology strongly support the notion that the *Tcf4*(+/−) mouse model the phenotype presented in PTHS. We next used the model to probe for potential downstream transcriptional consequences of PTHS, determine the effects on broad epigenetic regulation due to *Tcf4* haploinsufficiency, and screen potential neurotherapeutics.

Tcf4 Regulates Gene Transcription in the Hippocampus

Having characterized the deficits in learning and memory caused by *Tcf4* haploinsufficiency, it was of interest to identify downstream transcriptional targets of *Tcf4* in the hippocampus. We performed poly(A)+ RNA sequencing on hippocampal CA1 tissue from naive *Tcf4*(+/−) mice and WT controls. Using Cufflinks analysis, we determined 402 differentially expressed genes (DEGs) at a false discovery rate (FDR) of 0.05 (Figure 3A; Table S1). After annotating these DEGs through the Kyoto Encyclopedia of Genes and Genomes (KEGG) pathway database, we found that significant dysregulation occurred in biochemical pathways associated with neuronal plasticity, including axon guidance, cell adhesion, calcium signaling, and most prominently, neuroreceptors (Figures 3E and 3F). We hypothesized effects on cell adhesion pathways could be occurring through the neurexins *Nrxn1* and *Cntnap2*, given their potential relationship to *Tcf4*. However, the expression of these PTHS-associated genes was not affected by *Tcf4*(+/−) (Figure 3B). The binding partner for *Cntnap2*, *Cntn2*, was significantly downregulated.

More than half of the identified DEGs code for membrane-associated proteins that include a large concentration of neuroreceptors, many of which are upregulated (Figure 3B). This includes genes that govern the signaling of dopamine (*Drd1a*, *Cckbr*, and *Chrm4*), oxytocin (*Oxtr*), serotonin (*Htr2c*), glycine (*Glra2* and *Glra3*), and neuromedin B (Nmbr), suggesting *Tcf4* plays an important role in the negative regulation of these neurotransmitters in the hippocampus, although altered RNA stability or processing could also contribute to our observed effects. Conversely, other signaling pathways important in learning and memory are downregulated, such as NMDA receptor (NMDAR) subunit 2a (*Grin2a*), neuropeptide Y receptor (*Npy2r*), and a pair of lysophospholipid receptors (*Lpar1* and *S1pr5*). Another family of DEGs identified, and annotated by phenotype, is those genes that are known to regulate myelination (Figure 3B). Myelination states and oligodendrocyte differentiation have been implicated for some time in synaptic plasticity (Fields, 2005) and schizophrenia (Lee and Fields, 2009). All DEGs associated with myelination are downregulated.

Besides the large families of DEGs, other individual genes of interest were mined from the RNA sequencing (RNA-seq) data. Klotho (*Kl*), a membrane protein that has been identified as an enhancer of LTP in mice and associated with improved cognition in humans (Dubal et al., 2014), was found to be upregulated. *Arc* is a well-known immediate early gene (IEG) that plays an important role in synaptic plasticity, information processing, and memory

(Shepherd and Bear, 2011) and was found to be significantly downregulated. What precisely *Arc* deficiency means for *Tcf4*(+/−) naive mice is not entirely clear; however, *Arc* has been shown to negatively regulate AMPA receptor trafficking to the synapse and affect homeostatic scaling while neurons are held at rest with tetrodotoxin (Shepherd et al., 2006), which may help explain the observed enhancement in LTP. *Lefty1*, a member of the Nodal signaling pathway, is also significantly downregulated. *Lefty1* is predominantly expressed in the left hemisphere, including the hippocampus, and along with other members of the Nodal family, is responsible for many left-right asymmetries. Given that *Tcf4*(+/−) mice have weak front right paws and humans with PTHS have such stark language deficits, *Lefty1* is an interesting candidate as an effector of these phenotypes downstream from *Tcf4*.

Tcf4(+/−) Results in Altered DNA Methylation

DNA methylation has been shown to regulate chromatin organization, gene expression, synaptic plasticity, and memory and is a putative mechanism for long-term transcriptional regulation in neurons (Day et al., 2015; Gräff et al., 2011; Kennedy and Sweatt, 2016; Shin et al., 2014; Tsankova et al., 2007). To determine the potential dysregulation of genome-wide CpG methylation in the CA1 area of the hippocampus of *Tcf4*(+/−) mice, DNA extracted from the CA1 area was fragmented to lengths between 200 and 300 bp by sonication and methylated DNA sequestered by Methyl-CpG-binding domain protein 2 (MBD) association, which detects CpG dimethylation but not hemi-methylation or oxidized methylcytosine species (Aberg et al., 2012). These CpG-methylated DNA fragments (between 6% and 9% of all fragments) were then sequenced and mapped to the mouse genome (mm10) using the Bowtie 2.0 algorithm. In general, CpG methylation in the gene promoter inhibits gene transcription directly through the inhibition of transcription factor binding or by enhancing local chromatin organization around the transcription start site (TSS) via MBD binding and HDAC recruitment (Tan and Nakielny, 2006). Gene body CpG methylation is more enigmatic, with both transcript elongation and splicing effects documented (Jones, 2012). To first assess global CpG methylation trends, read density around genes was plotted (Figure 3C). *Tcf4*(+/−) mice have similar global methylation patterns across promoter regions but reduced methylation of across all gene bodies. However, changes in methylation are not uniform across all genes, and demethylation is significantly associated with upregulated DEGs, both at TSSs and gene bodies, but not with downregulated genes (Figure 3D).

To determine specific loci of differential genome methylation, individual sites of CpG methylation along the genome were identified using a genome-wide differential coverage analysis designed for Methyl-CpG-binding domain protein 2 sequencing (MBD-seq)-like data (Lienhard et al., 2014). The mm10 genome was divided into 300 nt windows, datasets were normalized using quantile normalization, and differential coverage was calculated using edgeR statistical analysis in the context of CpG density. Using this analysis, *Tcf4*(+/−) hippocampal tissue was found to have 734 differentially methylated regions (DMRs) at a FDR of 0.1 (Table S2). Select DMRs were then confirmed to have altered CpG methylation at the single nucleotide level using bisulfite sequencing from the same biological replicates (Figure S5).

HDAC Inhibition Normalizes LTP and Rescues Memory

Given the breadth of transcriptional dysregulation due to *Tcf4* haploinsufficiency, we considered therapeutic mechanisms that more broadly affect gene transcription. One such candidate that has already found success in improving learning and memory is HDAC inhibition, which has been shown to enhance LTP, improve learning and memory, and ameliorate memory deficits in models of Alzheimer's disease (Fischer et al., 2007; Kilgore et al., 2010). This was particularly appealing given the role *Tcf4* plays in regulating histone acetylation by attracting either HATs or an HDAC-bound nuclear suppressor complex to TSSs. The HDAC inhibitor CI-994 has been shown to improve memory extinction after threat recognition training in mice (Gräff et al., 2014). In this prior study, mice were trained and treated with CI-994 and RNA-seq was performed on tissue extracted from the hippocampus post-extinction. To assess the therapeutic potential of HDAC inhibition for PTHS, the published gene expression profiles from CI-994 treatment were compared to our newly acquired data. Figure 3G shows the significant overlap ($p < 2.7 \times 10^{-76}$, representation factor = 11.8) of 97 DEGs between the *Tcf4*(+/−) and CI-994 datasets (Table S3). Nearly one-quarter of the genes dysregulated in the *Tcf4*(+/−) mice are also regulated by HDAC inhibition. The strong negative correlation between *Tcf4*(+/−) and CI-994 DEGs ($R^2 = 0.72$) suggests HDAC inhibition is a viable avenue for correcting a large percentage of transcriptional dysregulation associated with *Tcf4* haploinsufficiency.

To determine whether HDAC inhibition would be sufficient to normalize synaptic plasticity in the CA1 area of the hippocampus of *Tcf4*(+/−) mice, LTP studies of Schaffer collaterals were performed after incubating the hippocampal slice with the HDAC inhibitor Trichostatin A (TSA) for 20 min before theta burst stimulation (Figures 4A–4C). In other models with cognitive deficits, and with WT mice, HDAC inhibition has been associated with enhanced LTP in the CA1 area, an effect that can be blocked by inhibitors of transcription and those of active DNA methylation (Miller et al., 2008). It was therefore unclear whether TSA treatment would similarly increase the already enhanced LTP observed in *Tcf4*(+/−) mice. Surprisingly, TSA treatment significantly reduced LTP in the *Tcf4*(+/−) hippocampus, even though there is a measured increase in LTP for TSA-treated WT controls. This observed reduction in LTP mediated by HDAC inhibition in the CA1 area of the *Tcf4*(+/−) mice, albeit unexpected, had the effect of normalizing the LTP magnitude to that of untreated WT controls (Figure 4C).

These LTP results prompted us to test the hypothesis that HDAC inhibition would be effective in improving cognition in PTHS model mice. *Tcf4*(+/−) mice were treated subchronically with suberoylanilide hydroxamic acid (SAHA; vorinostat, Zolinza) at 25 mg/kg once per day intraperitoneally (i.p.) for 10 days before behavioral assessment. SAHA did not measurably affect activity or anxiety in WT or *Tcf4*(+/−) mice (Figures 4D and 4E). The SAHA-treated *Tcf4*(+/−) mice, along with vehicle and WT controls, were then submitted to the threat recognition training protocol described earlier, and contextual and cued tests were performed 24 hr after training (Figures 4F and 4G). Subchronic administration of SAHA was sufficient to rescue memory-associated freezing in *Tcf4*(+/−) mice to levels observed in the contextual and cued tests for WT mice. Altogether, these

results indicate that HDAC inhibitor treatment improves learning and memory in *Tcf4*(+/−) mice through the normalization of synaptic plasticity.

The enhancement in LTP and the strong correlation between the *Tcf4*(+/−) DEGs and those genes differentially expressed by HDAC inhibition after memory recall (Figure 3G) led us to wonder whether learned information was being at least temporarily consolidated but rendered inaccessible or impermanent by hyperplasticity. Consequently, *Tcf4*(+/−) mice were trained using the trace threat recognition protocol, in which a white noise tone (CS) is presented 15 s before a 0.5 mA foot shock (US) for a total of three pairings (Figure 4H). Trace conditioning caused by this protocol is optimal in this case, because it has been shown to be dependent on NMDAR activity in the CA1 area (Quinn et al., 2005). A cue test was then performed 24 hr after training to assess memory recall, after which *Tcf4*(+/−) mice were treated daily with SAHA for 10 days before being submitted to a second cue test. *Tcf4*(+/−) mice exhibited reduced freezing when presented with the CS in a novel context 24 hr after training (Figure 4I); however, after SAHA treatment, memory was rescued to WT levels and significantly increased over *Tcf4*(+/−) vehicle controls (Figure 4J). This HDAC inhibitor-mediated restoration of a previously irretrievable memory is surprising but not unprecedented—similar results were obtained in studies of a mouse neurodegeneration model (Fischer et al., 2007). Overall, these data suggest a strong potential for HDAC inhibitors as therapeutics for improving cognition and memory recall in PTHS.

Tcf4(+/−) Affects the Expression and DNA Methylation of Memory-Associated Genes

Several *Tcf4*(+/−) DEGs, notably *Arc* and *Grin2a*, are known to be important in long-term memory formation. However, to better understand the scope *Tcf4* plays in regulating memory-associated genes and to test whether SAHA affects the expression of these genes in the hippocampus, a series of next-generation sequencing experiments was conducted on *Tcf4*(+/−) hippocampal tissue shortly after threat recognition training, with and without the administration of SAHA. *Tcf4*(+/−) and WT were treated with SAHA or vehicle for 10 days and then either trained using the trace threat recognition protocol described previously or kept naive. The mice were sacrificed 1 hr after training, and RNA and DNA were extracted from the CA1 region of the hippocampus (Figure 5A). As with the untreated and untrained sequencing experiments, poly(A)+ RNA-seq and MBD-seq were performed to determine the genome-wide changes in gene transcription and DNA methylation induced by experiential learning and modulated by subchronic SAHA injection, as well as how these dynamics are affected by *Tcf4*(+/−).

First, an analysis of DEGs between the *Tcf4* (+/−) naive vehicle and WT naive vehicle groups was performed to validate the original RNA-seq study. Comparing the original 402 *Tcf4*(+/−) DEGs to the 529 *Tcf4*(+/−) naive vehicle DEGs shows a highly significant and correlative overlap of 199 genes that were independently identified in both sequencing experiments (Figure 5B). This degree of similarity for the untreated and vehicle *Tcf4*(+/−) groups versus their respective controls demonstrates the reproducibility of these sequencing experiments. In addition, Fischer's meta-analysis was performed across these datasets to combine p values and generate a more confident list of 678 genes dysregulated in the hippocampal CA1 area of *Tcf4*(+/−) mice (Table S4).

These data also allow the identification of 1,517 memory-associated genes that have altered transcription after threat recognition training by comparing the expression of the WT naive vehicle group to that of WT trained vehicle group (Figure 5C; Table S5), including well-characterized IEGs that are upregulated shortly after learning, such as *Arc*, *Fos*, and *Egr2*, and genes that are downregulated after experiential learning, such as *Grin2a* and *Malat1*. Cross-comparing the DEGs identified between each of the seven most relevant pairwise comparisons (trained, WT trained vehicle versus WT naive vehicle; SAHA, WT naive SAHA versus WT naive vehicle; trained SAHA, WT trained SAHA versus WT naive SAHA; *Tcf4*(+/−), *Tcf4*(+/−) naive vehicle versus WT naive vehicle; *Tcf4*(+/−) trained, *Tcf4*(+/−) trained vehicle versus *Tcf4*(+/−); *Tcf4*(+/−) SAHA, *Tcf4*(+/−) naive SAHA versus *Tcf4*(+/−) naive vehicle; *Tcf4*(+/−) trained SAHA, *Tcf4*(+/−) trained SAHA versus *Tcf4*(+/−) naive SAHA) in a chord diagram illustrates those DEG lists with high degrees of overlapping gene identities (Figure 5D; Table S6). The strongest degree of overlap is between the two trained gene lists for WT and *Tcf4*(+/−), demonstrating that 414 of the 1,517 memory-associated genes are also being activated in *Tcf4*(+/−) mice after experiential learning. However, the association that stood out the most was the 217 DEGs that overlap between the trained and the *Tcf4*(+/−) gene lists ($p = 3.4 \times 10^{-87}$), confirming that *Tcf4* regulates a large number of genes that are actively regulated by learning. Both the trained and the *Tcf4*(+/−) DEGs are also closely related to those genes with expression altered by treatment with SAHA, highlighting the interconnected relationship among *Tcf4*, HDAC inhibition, and memory formation at the level of gene expression.

Analyzing the expression of individual genes across these datasets, especially *Tcf4*(+/−) DEGs, should provide insight into how HDAC inhibition, an epigenetic therapy that broadly affects transcription, improves learning and memory in *Tcf4*(+/−) mice (Figure 5E). *Tcf4* trends toward decreased expression after training in both WT and *Tcf4*(+/−) mice (Fischer's combined $p < 0.02$). SAHA administration does not profoundly affect Tcf4 expression in WT or *Tcf4*(+/−) mice; however, there are small, yet significant, changes in *Tcf4* expression in *Tcf4*(+/−) mice after training compared to vehicle controls at the level of individual transcripts (Figure S6). *Grin2a*, downregulated in *Tcf4*(+/−) mice, is also downregulated after training (Figure 5E). SAHA administration significantly increases *Grin2a* gene expression in *Tcf4*(+/−) mice compared to vehicle controls. However, not all *Tcf4*(+/−) DEGs responded to SAHA treatment. For example, *Arc*, a downregulated *Tcf4*(+/−) DEG and an IEG, is unaffected by SAHA in *Tcf4*(+/−) mice. *Malat1*, an upregulated *Tcf4*(+/−) DEG and non-coding RNA that is downregulated after training, is similarly unresponsive to SAHA. In addition, both *Arc* and *Malat1* respond to training at similar levels in WT or *Tcf4*(+/−) mice, demonstrating that their function as memory-associated genes is not impaired. Several *Tcf4*(+/−) DEGs with expression unaffected by training had their expression levels rescued by SAHA (Figure 5E). *Lefty1* and *Wbscr17*, both downregulated in *Tcf4*(+/−) mice, are upregulated by SAHA after training. Many extracellular matrix genes were identified as downregulated in *Tcf4*(+/−) mice, and the upregulated expression of two collagen subunits, *Col6a1* and *Col23a1*, was ameliorated by SAHA (Figure 5E).

These data also reveal a class of *Tcf4*(+/−) DEGs dysregulated after experiential learning but not identified as dysregulated at baseline. *Fos*, a transcription factor and IEG associated with memory formation in the hippocampus (Countryman et al., 2005), and *Tet2*, a member of

the 5-methyl cytosine hydroxylase family of TET enzymes that control active DNA demethylation that is downregulated after training (Kaas et al., 2013), are both overexpressed in *Tcf4*(+/−) mice compared to WT controls (Figure 5E). *Npas4* and *Dusp1* are IEGs that are upregulated after training (Figure 5F). While these genes do not have dysregulated expression in the naive *Tcf4*(+/−) groups compared to naive WT controls, they are expressed at relatively higher levels in *Tcf4*(+/−) mice after training.

Many genes with altered expression after training are similarly affected by SAHA administration. Of the 712 genes with altered expression due to SAHA treatment, 347 overlap with the trained gene list ($p = 1.1 \times 10^{-225}$). In most cases, SAHA drives the expression, increased or decreased, in the same direction that these genes respond to training (Figure 5G). We find this result fascinating given the wide applicability of SAHA as a cognitive enhancing drug in animal models, and the degree of overlap between the SAHA and the trained datasets is even more remarkable when considering that we are examining just one time point after threat recognition training. Genes with expression altered by training that are also differentially expressed between the *Tcf4*(+/−) trained vehicle and the WT trained vehicle, notably *Npas4* and *Dusp1* (Figure 5F), are also significantly affected by SAHA in *Tcf4*(+/−) mice. Of the 560 genes differentially expressed between *Tcf4*(+/−) and WT mice after training, 102 genes are significantly altered in the *Tcf4*(+/−) trained SAHA group (Figure 5H), many of which are memory-associated genes (Figure 5H, filled dots). This predominately inverse relationship demonstrates how SAHA ameliorates the expression of memory-associated genes that are dysregulated in *Tcf4*(+/−) mice shortly after training, and it identifies a list of genetic targets through which SAHA may act to improve learning and memory in *Tcf4*-deficient mice.

To identify genes with highly significant regions of altered CpG methylation, Fischer's meta-analysis was performed, combining the power of the original *Tcf4*(+/−) MBD-seq experiment with that of the *Tcf4*(+/−) naive vehicle group compared to WT controls. This method identified 707 reproducible and highly significant *Tcf4*(+/−) DMRs that reside within annotated genes. It is also known that experiential learning induces changes in DNA methylation, and we identified 314 DMRs associated with genes when comparing the WT trained vehicle and the WT naive vehicle datasets (Table S7). Changes in CpG methylation incurred by *Tcf4*(+/−) had significant overlap with loci that had differential CpG methylation induced by training for both WT and *Tcf4*(+/−) trained groups (Figure 6A). Unlike SAHA-treated WT mice, which had almost no changes in CpG methylation compared to vehicle controls, SAHA-treated *Tcf4*(+/−) mice had 88 gene-associated DMRs that also overlapped significantly with *Tcf4*(+/−) DMRs.

An important question to address is whether these identified changes in CpG methylation at genes are associated with changes in transcription. Figure 6B shows the cross-comparison of the DEGs and DMRs for each of the seven most relevant pairwise comparisons, with all significantly overlapping datasets displaying the number of genes in common on the corresponding list of DEGs and gene-associated DMRs. There are several significant associations, notably for changes in expression and DNA methylation between the trained and the *Tcf4*(+/−) gene lists, but the highest degree of overlap is between trained DEGs and *Tcf4*(+/−) genes containing DMRs ($p = 9.6 \times 10^{-4}$). CpG methylation is often an inhibitory

epigenetic mark with distinct patterns of methylation between genes that are expressed and those that are silenced (Figure 6C). These data also demonstrate a difference in methylation patterns around genes that are upregulated post-training versus genes that are downregulated, with upregulated genes having significantly greater levels of gene body CpG methylation, despite similar methylation levels at the TSS, compared to downregulated genes (Figure 6D). Given that *Tcf4*(+/−) DMRs are disproportionally associated with trained DEGs, it was expected that methylation patterns around these genes would be systematically altered. There is global demethylation of upregulated trained DEGs in the *Tcf4*(+/−) group but no significant difference in the methylation patterns around genes that are downregulated after training. The demethylation of these upregulated trained DEGs correspond with the general trend that these genes exist in a state of increased expression at baseline in *Tcf4*(+/−) hippocampal tissue (Figure 6E).

Hdac2 Knockdown Is Sufficient to Rescue Learning and Memory

SAHA, like many small-molecule HDAC inhibitors, has promiscuous HDAC subtype selectivities. To identify SAHA's functional target for improving learning and memory in the *Tcf4*(+/−) system, an interactome network was created based on the original *Tcf4*(+/−), *Tcf4*(+/−) naive vehicle, and *Tcf4*(+/−) trained vehicle DEGs versus WT controls (Breuer et al., 2013). This network of gene product interactions (Figure 6F) identifies nodes, individual proteins that have a high degree of interconnectivity between and within the list of DEGs, to identify key pathways of dysregulation. For the *Tcf4*(+/−) system, it is therefore not surprising that *Tcf4* is identified as a top node of dysregulation that is downregulated overall (Figure 6G). The top downregulated node is *Ubc*, a polyubiquitin precursor gene. *Ubc* is interesting given the similarities in phenotype between PTHS and Angelman syndrome, caused by mutations in the ubiquitin ligase *Ube3a*. The top upregulated node is *Hdac2*, an HDAC isoenzyme that is present in high levels in the CNS and has previously been implicated as an epigenetic modifier that plays an important role in regulating synaptic plasticity and memory formation (Guan et al., 2009). We hypothesized that upregulation of *Hdac2* and associated genes in the *Tcf4*(+/−) system could be driving the behavioral deficits in learning and memory and HDAC2 protein could be the functional target of SAHA to rescue those behaviors in *Tcf4*(+/−) mice. To test this idea, we designed antisense oligonucleotides (ASOs) to selectively target *Hdac2*.

Phosphorothioate and 2′-*O*-methoxyethyl (2′-MOE) modified ASOs have been shown to elicit selective and prolonged RNA knockdown, remain active in the CNS for several months, and rescue deficits in mouse models for Angelman syndrome and Huntingdon's disease (Kordasiewicz et al., 2012; Meng et al., 2015) through hybridization and degradation of target RNA by recruitment of RNase H (Wu et al., 2004). To test whether *Hdac2* could be a therapeutic target for improving cognition in PTHS, approximately 500 ASOs were designed against the full rat *Hdac2* gene, with higher density of ASOs targeting exonic regions (Figure S7), and were evaluated for *Hdac2* knockdown at L2-RYC cells. The most active ASOs were taken into a four-point dose response in L2-RYC cells, and five of the most potent ASOs that were complementary to mouse *Hdac2* were injected intracerebroventricularly (ICV) into C57BL/6 mice at a dose of 300 μg. Two weeks after

dosing, RNA was extracted from cortex, hippocampus, and spinal cord and *Hdac2* RNA reduction was measured by qPCR (Figure S7).

HDAC2-ASO1, which targets the 3′ UTR (3′ UTR) of *Hdac2*, was chosen from the screen and administered to the CNS of 2-month-old *Tcf4*(+/−) mice through a single ICV injection to the lateral ventricle, along with WT and control ASO groups, before entering a behavioral battery (Figure 7A). As was similarly observed with the treatment of SAHA, there was no effect on activity or anxiety due to *Hdac2* knockdown in the open field (Figures 7B and 7C); however, HDAC2-ASO1 significantly improved performance in each of the three memory tasks we evaluated. In OLM, HDAC2-ASO1-treated *Tcf4*(+/−) mice showed highly significant improved discrimination for the object placed in the novel location (Figure 7D). HDAC2-ASO1-treated *Tcf4*(+/−) mice also showed improved training and significantly increased target quadrant localization and platform crossings in the MWM (Figures 7F–7H). Lastly, HDAC2-ASO1-treated *Tcf4*(+/−) mice demonstrated improved contextual threat recognition 24 hr after training compared to a control ASO (Figure 7E), meaning that in all three paradigms, the behavior of treated *Tcf4*(+/−) mice was rescued to the level of that of WT control ASO. HDAC2-ASO1-treated WT mice show significantly improved 24 hr OLM, suggesting that *Hdac2* knockdown improves cognition in some tasks outside of the *Tcf4*(+/−) system, as has been found with the extinction of recent memories (Gräff et al., 2014).

Hippocampi were harvested 3 months after ICV injection, and RNA was extracted to confirm knockdown of the *Hdac2* message and protein (Figure 7I; Figure S7). *Hdac2* expression was knocked down 55% in both WT and *Tcf4*(+/−) mice treated with HDAC2-ASO1, while *Hdac1* expression was not measurably affected. One explanation as to how *Hdac2* inhibition might rescue memory in *Tcf4*(+/−) mice is by the upregulation of *Tcf4* expression directly, because subchronic SAHA upregulated some *Tcf4* transcripts, and *Tcf4*(+/−) mice treated with HDAC2-ASO1 had significantly increased *Tcf4* expression in the hippocampus compared to control ASO. *Tcf4* expression is not altered in cortex or cerebellum despite comparable levels of *Hdac2* knockdown (data not shown).

To determine whether *Hdac2* knockdown was sufficient to normalize the expression of candidate genes found to be dysregulated by RNA-seq, the expression of *Kl*, *Arc*, *Lefty1*, and *Grin2a*, as well as NMDAR subunit 2b (*Grin2b*) as a negative control, was assessed by PCR analysis (Figure 7I). *Hdac2* knockdown, like SAHA administration, was unable to significantly affect the expression of *Kl* and *Arc*. Meanwhile, the expression of *Lefty1* and *Grin2a*, both downregulated at baseline and increased by SAHA, responded to *Hdac2* knockdown with significant increases in transcription. *Grin2b* does not have a putative Tcf4 binding site within its promoter, is not dysregulated by *Tcf4*(+/−), and is not affected by *Hdac2* knockdown. *Kl*, *Arc*, *Lefty1*, and *Grin2a* all have putative *Tcf4* binding sites within 3 kb of their TSSs, suggesting that the dysregulation of some DEGs, such as *Kl* and *Arc*, are no longer caused by reduced *Tcf4* concentration, because increasing *Tcf4* expression does not measurably affect their transcription. The expression of *Tet2*, which catalyzes the removal of methyl marks from DNA and is overexpressed in *Tcf4*(+/−) hippocampal tissue, was also significantly decreased by *Hdac2* knockdown, as with SAHA treatment.

However, further experimentation is necessary to determine whether normalizing *Tcf4* expression post-developmentally is sufficient to improve cognition. One possibility is that HDAC inhibition improves learning and memory in *Tcf4*(+/−) mice predominately through increased histone acetylation at the *Tcf4* gene locus, resulting in its increased expression. Previously reported data demonstrate significant TSA-induced hyperacetylation of histone 3 at *Tcf4* and an enhancer region upstream from the TSS (Lopez-Atalaya et al., 2013). However, SAHA only marginally increases the expression of some *Tcf4* transcripts while still providing cognitive enhancement. In addition, HDAC inhibition has been shown to improve learning and memory outside the *Tcf4*(+/−) system (Gräff and Tsai, 2013). HDAC inhibition could be beneficial in a mostly *Tcf4*-independent fashion by affecting global histone acetylation levels, and HDAC2-ASO1 enhances H4K12 acetylation in cultured hippocampal neurons (Figure S8) but not H3 acetylation, matching global effects observed in *Hdac2* knockout hippocampal tissue (Guan et al., 2009). Finally, one explanation as to why the effects of HDAC inhibition are large in the *Tcf4*(+/−) system is that TSSs that contain *Tcf4* binding sequences are acetylated by TSA to a greater level than sites that do not.

DISCUSSION

PTHS has compelling attributes in terms of human cognitive function, being associated with pronounced memory deficits, autistic behaviors, and an almost complete lack of language development. Thus, understanding the roles and function of *Tcf4* in the CNS is highly significant with respect to human language and auditory cognition, memory function, autism spectrum behavior, and schizophrenia susceptibility. Despite the clear importance of *Tcf4* function in the human CNS, the basic neurobiology of *Tcf4* had previously been only sparsely studied. Thus, for these studies, we used a genetically engineered mouse model to assess the role of *Tcf4* in memory, social interactions and communication, hippocampal synaptic plasticity, and epigenomic and transcriptional regulation in the CNS. Moreover, while it is well-established that regulation of gene transcription is necessary for late-phase LTP and long-term memory consolidation, relatively few specific transcriptional regulators have been firmly tied to these phenomena to date. Our studies add the *Tcf4* transcription factor to the emerging list of transcriptional and epigenetic regulators relevant to CNS synaptic plasticity and memory.

This study characterizes *Tcf4*(+/−) mice as a model system for PTHS, implicates *Tcf4* in the regulation of gene transcription in the CNS, and identifies HDACs, specifically *Hdac2*, as potential neurotherapeutic targets for PTHS. *Tcf4*(+/−) mice demonstrate behavior that is consistent with the cognitive and motor dysregulation associated with PTHS. *Tcf4*(+/−) mice exhibit statistically significant learning deficiencies in cued and contextual threat recognition and deficits in spatial learning and memory as tested by the MWM and OLM. *Tcf4*(+/−) mice also demonstrate motor and balance asymmetry, favoring their front left paw when resting and ambulating, and have significantly reduced hindlimb grip strength. We interpret these results as being consistent with the learning disability and deficits in gross motor control associated with PTHS clinically. *Tcf4*(+/−) mice are also averse to social interaction, and *Tcf4*(+/−) pups (P3) elicit fewer USVs and at lower pressures compared to WT pups, phenotypes associated with genes connected to language impairments and other ASDs.

These findings broadly implicate the *Tcf4* transcription factor as a potent regulator of cognition in the domains of learning, memory, and social interactions. Moreover, based on both these mouse studies and studies in human PTHS patients, *Tcf4* is a viable candidate as a language-associated gene.

The development of new valid targets for therapeutics targeting PTHS and other ASDs is a pressing biomedical issue. In our studies, we undertook preclinical proof-of-principle studies and evaluated whether HDAC inhibitors could ameliorate memory deficits exhibited by a mouse model of PTHS. The rescue of the threat recognition memory deficits observed in *Tcf4*(+/−) mice by treatment with SAHA has substantial implications for PTHS and other language disorders. Besides the rescue of threat recognition memory by subchronic SAHA treatment before training, we observed the retrieval of a memory by SAHA treatment post-training, even after the memory was already demonstrated to be inaccessible. This is not unprecedented for HDAC inhibitors; a similar effect of HDAC inhibition on cryptic memories has been demonstrated in a neurodegeneration mouse model (Fischer et al., 2007). However, the observation is decidedly idiosyncratic. These data imply that the association between the CS and the US could be at least temporarily consolidated and that HDAC inhibition leads to the acquisition of the otherwise obstructed memory trace.

The CNS gene targets of *Tcf4* were almost completely unknown, and we addressed this question using unbiased next-generation sequencing, combining MBDseq and mRNAseq approaches. Using these approaches, we not only identified a large number of transcriptional changes triggered by *Tcf4* deficiency in the CNS, but we also identified several gene targets that had previously been functionally linked to the regulation of synaptic plasticity and memory formation. We also used MBD-mediated gene pull-down coupled with large-scale parallel sequencing approaches to identify candidate genes with dysregulated CpG methylation in PTHS. This aspect of our studies was motivated by the discovery of a role for epigenetic molecular mechanisms in synaptic plasticity, learning, and memory (Day et al., 2015). An emerging idea is that the regulation of chromatin structure, mechanistically via histone modifications and direct chemical modification of DNA, contributes to long-lasting behavioral change. Our observations of epigenetic and transcriptional alterations regulated by loss of *Tcf4* function are consistent with this fundamental hypothesis of a role for DNA methylation in regulating memory and cognition both in laboratory mouse models and in human PTHS patients.

Specifically, a set of genome-wide sequencing experiments of hippocampus-derived mRNA and methylated DNA from *Tcf4*(+/−) and WT naive mice, before or shortly after threat recognition training and with or without SAHA treatment, was performed to identify genes with altered transcription and DNA methylation following experiential learning and/or SAHA administration. These data provide insight into the transcriptional regulation of memory formation by identifying the following: genes recruited 1 hr after experiential learning (memory-associated genes), increased CpG methylation at genes upregulated compared to downregulated after learning, SAHA as a modulator of memory-associated gene expression, and how these mechanisms are altered in the *Tcf4*(+/−) system and relate to PTHS. *Tcf4*(+/−) causes dysregulation in the expression of neuroreceptors, including *Grin2a*; activity-dependent genes, such as *Arc*, *Dusp1*, *Egr2*, *Fos*, and *Npas4*; and regulators

of synaptic plasticity, such as *Kl*. In addition, the epigenetic modifier *Tet2* was found to be relatively overexpressed after training compared to WT controls. Our data also revealed that *Tcf4*(+/−) causes decreased CpG methylation at genes with upregulated transcription following experiential learning and that these memory-associated genes were correspondingly upregulated at baseline in *Tcf4*(+/−) mice. *Tcf4* may govern the methylation of genes with increased transcription after learning through the negative regulation of *Tet2* expression, shown to be associated with the demethylation of gene bodies (Huang et al., 2014), or the demethylation of memory promoting genes could be a compensatory mechanism. SAHA causes a significant increase in gene body methylation in *Tcf4*(+/−) but not WT mice, which corresponds with a blunting of transcription for these genes post-training (Figure 5H).

Using the catalog of sequencing experiments presented here, we then generated an interactome network to identify key dysregulated pathways in the *Tcf4*(+/−) model system. This led to the identification of upregulated *Hdac2* activity, as well as gene products known to interact with *Hdac2*. To test whether a reduction of HDAC2 protein was sufficient to improve learning and memory in *Tcf4*(+/−) mice, 500 ASOs targeting the *Hdac2* locus were design and evaluated. A single ICV injection of a long-lasting HDAC2 ASO was found to be sufficient to rescue spatial memory in the OLM and MWM tasks, as well as threat recognition memory to WT levels. In addition, *Hdac2* knockdown normalized the expression of *Tcf4*(+/−) DEGs, such as *Grin2a*, *Tet2*, and *Lefty1*, as well as directly increasing *Tcf4* expression.

Lastly, it was found that *Tcf4*(+/−) causes enhancement of LTP at Shaffer collaterals in the CA1 area. This is not novel for models with impaired memory (Gu et al., 2002); however, the observation that HDAC inhibition attenuates LTP in the *Tcf4*(+/−) hippocampus is unprecedented. Prior genome-wide expression analysis revealed increased *Kl* results in enhanced LTP and alters NMDAR subunit composition by upregulating *Grin2b* and ramping up the *Grin2b*/*Grin2a* rheostat (Dubal et al., 2014), which decreases over the course of CNS development and has been shown to play a role in governing decreased excitability of hippocampal neurons post-learning (Abraham, 2008; Liu et al., 2004; Yashiro and Philpot, 2008). Because *Grin2a*-containing NMDARs produce shorter currents compared to those with *Grin2b* and NMDAR activation is necessary for the establishment of LTP and some forms of LTD, the ratio of *Grin2b*/*Grin2a* is seen as a mechanism by which a neuron can modulate its intrinsic excitability. *Tcf4* was shown to be a regulator of intrinsic excitability in cortical neurons (Rannals et al., 2016). The pharmacological normalization of LTP via HDAC inhibition and the significant increase in *Grin2a* expression by both SAHA treatment and *Hdac2* knockdown, coupled with the rescue of learning and memory phenotypes in Tcf4(+/−) mice, strongly support the potential of using neuroepigenetic therapies, specifically targeting HDAC activity, for the treatment of PTHS.

The observed therapeutic effects of HDAC inhibitors post-developmentally in young adult mice suggest a shift in thinking about neurodevelopmental disorders such as PTHS. The genetic basis of PTHS is mutation or deletion of the *Tcf4* gene and resultant disruption of normal *Tcf4* transcription factor function. *Tcf4* is present throughout development and is present in the fully developed adult CNS. However, it is unclear whether PTHS is caused

exclusively by disruption of *Tcf4* function during development or whether loss of *Tcf4* in the mature CNS might also contribute to neurobehavioral and cognitive dysfunction in PTHS patients. Data from studies of a number of different developmental disorders, such as Rett, Angelman, and fragile X mental retardation, have begun to suggest that loss of normal gene function in the post-developmental nervous system contributes to cognitive and neurobehavioral dysfunction in these disorders. Our finding of ameliorative effects of HDAC inhibition post-developmentally in our PTHS mouse model is consistent with this line of thinking concerning *Tcf4* function in the CNS.

In summary, *Tcf4* is a transcription factor that remains enigmatic, and its precise roles in schizophrenia, autism, and cognition are yet unclear. However, the present study sheds considerable light onto the basic underlying neurobiology and biochemistry of *Tcf4* haploinsufficiency. Moreover, we provide evidence that certain cognitive aspects of PTHS can be ameliorated, even post-developmentally, through a neuroepigenetic therapy such as HDAC inhibition. This study also implicates epigenetic mechanisms regulated by *Tcf4*, specifically DNA methylation and histone acetylation, in governing CNS plasticity and major subdomains of cognitive function, including memory, social interactions, and auditory communication.

EXPERIMENTAL PROCEDURES

All experiments were performed and analyzed by those unaware of genotype or treatment.

Tcf4(+/−) Mice

Heterozygous male B6;129-Tcf4tm1Zhu/J mice were acquired from The Jackson Laboratory (stock #013598) and breed with female B6129SF1/J mice (stock #101043) to produce *Tcf4*(+/−) and WT littermates. All experiments were performed on male mice between 2 and 3 months of age, unless otherwise noted. All procedures were performed with Institutional Animal Care and Use Committee (IACUC)-approved protocols and conducted in full compliance with the Association for Assessment and Accreditation of Laboratory Animal Care (AAALAC).

Behavior

Open Field—Open-field behavior was examined for 30 min using the infrared photobeam Med Associates system for mice.

Elevated Plus Maze—Elevated plus maze behavior was examined for 5 min using the near-infrared backlit maze for mice from Med Associates.

Dynamic Weight Bearing—Animals were allowed 10 min to habituate undisturbed in the commercially available dynamic weight bearing device (Bioseb). Following this habituation period, 3 min of video was recorded and analyzed by the connected computer program (Advanced Dynamic Weight Bearing software; Bioseb). Three states were differentiated (four paws, three paws, and rearing on two paws), and recordings of the surface area (in square millimeters) and weight (in grams) applied to each paw in contact with the sensor pad during this posture were automatically computed.

CatWalk—Static and dynamic locomotor activity were assessed using the CatWalk gait analysis system (CatWalk 9.1; Noldus Information Technology), as previously described (Hetze et al., 2012). Briefly, the animals traversed an elevated glass walkway (130 × 21.5 × 0.6 cm) encased with dark plastic walls spaced 5 cm apart in a darkened room. Red fluorescent light illuminates the walkway, and green light enters at the edge of the glass plate and is internally reflected within the glass walkway. Scattering of the light occurs when the paw surface contacts the glass walkway, thereby producing paw prints. Recordings of paw prints were made with a high-speed camera mounted underneath the glass walkway and analyzed on a connected computer. Mice were allowed three training trials on one training day before assessment. For experimental inclusion, animals were required to make three full passes on the instrument (two right to left and one right to left) on the training day. The average of three compliant trials (minimum duration, 0.5 s; maximum duration, 5.0 s; maximum speed variation, 60%) on the testing day (two traveling from right to left and one from left to right) was found from the data. Data were analyzed using CatWalk 9.1 software. The >190 parameters analyzed (previously described by Hamers et al., 2006) included those describing individual paws, paw print positioning, and the temporal relationship between paw prints. Significant findings are reported in Figure S1 and include definitions of each gait parameter.

Grip Strength—Neuromuscular function of the forelimbs and hindlimbs was tested with a grip strength meter (San Diego Instruments). To assess forelimb grip strength, the meter was positioned horizontally, the mice were held by the tail and lowered toward the apparatus, and then they were allowed to grasp the smooth metal grid (forelimbs only) and were pulled backward in the horizontal plane. To assess hindlimb grip strength, we scruffed the mice by the back of the neck, held them by the tail, and lifted them into an upright position. Then, the mice were lowered toward the apparatus, allowed to grasp the smooth metal grid (hindlimbs only), and pulled backward in the horizontal plane. The force applied to the grid at the moment the grasp was released was recorded as the peak tension (in newtons) and normalized to the animal's weight. Grip strength was measured in triplicate and averaged.

Horizontal Ladder—Motor ataxia was assessed with a commercially available horizontal ladder (Bioseb). Mice were allowed three training trials on three separate training days. For experimental inclusion, animals were required to cross the ladder in under 90 s on a minimum of two training trials on the final training day. Data from the final testing day are the average of two trials.

Rotating Rod—Gross motor coordination and memory were assessed by the ability to balance on a rotating and progressively accelerated rod. Using a Five Station Rota-Rod Treadmill (Med Associates), latency to fall was measured over a 5 min trial window as the rod was lineally accelerated from 4 to 40 rpm. Four trials were performed each day, with a minimum of 1 hr between trials, for a total of 12 trials.

Social Interaction—The three-chamber social interaction test consists of a 40 × 50 cm field made of opaque polyurethane divided into three equally proportioned chambers by clear plastic walls with a 5 × 5 cm passage between them, with two equivalent distal

chambers and one center chamber linking them together. The two distal chambers each contain a single cylindrical steel cage, one of which holds a novel mouse and the other of which is empty. The test mouse is habituated to the chamber and steel cages for 10 min before testing (Figure S2). Then, a novel mouse is placed in out of the two cages at random, the test mouse is reintroduced to the center chamber, and the time spent in each chamber is recorded over a 10 min trial.

Grooming—Mice were placed in an empty home cage with fresh bedding and allowed to habituate for 10 min. Then, they were observed for a 10 min block and the time spent grooming was recorded.

Startle Reflex and Prepulse Inhibition—The startle response to 120 dB white noise and its inhibition by a prepulse was examined using the Acoustic Startle Reflex Package for mice from Med Associates. A 4 kHz prepulse was presented 0, 4, 8, and 16 dB above a 65 bD background white noise.

USVs and Distress Calls—Pups (P3, P5, P7, P9, and P11) were removed from the home cage and placed into a soundproof chamber, and USVs were detected over a 5 min period using an Ultrasonic Vocalization Detector from Med Associates. Ultrasonic distress calls were elicited by lifting and holding the pup by hand for 30 s after the 5 min USV detection period.

OLM—Mice were trained for 10 min with two 50 ml beakers and one black line spatial cue in a 10 × 10 × 12 in (x, y, z) opaque polyurethane open box containing autoclaved bedding. Before training, mice were habituated to the box and bedding without objects for 4 days, 5 min each day. Then, 24 hr after training, one beaker was moved to a novel location and the mice were tested for 5 min. Videos were scored by hand and blind to subject identity, and object interaction was scored as previously described (Haettig et al., 2011).

MWM—Mice were trained in a 135 cm diameter pool made opaque with water-soluble non-toxic white paint and a square 10 × 10 cm platform placed 27 cm from the northwest wall of the pool and submerged 5–7 mm below the surface of the water. Four distinct visual cues were placed on the north, south, east, and west walls. Mice were trained with four trials a day (block), separated by 1 hr between trials, for a total of 4 days. Mice were placed in the pool at four points, randomly for each trial, and latency to find the platform was measured. Then, 24 hr after the final day of training, the platform was removed from the pool and mice were test in a 60 s trial for time spent in the quadrant previously containing the platform (target quadrant) and the number of times the mouse swam over the exact location of the platform (platform crossings). Finally, the spatial cues were removed from the wall and a small visual cue (6 inch flag) was placed directly on the platform. Eight trials of visible-platform training (four trials per day) were conducted, and latencies to the platform were recorded.

Threat Recognition—Training consisted of a 2 min habituation period followed by three 20 s, 80 dB white noise cues (CS) spaced 100 s apart and each followed 15 s later by a 1 s, 0.5 mA foot shock (US). The animals remained in the chamber for an additional minute

before being returned to their home cage. For the 24 hr contextual test, mice were reintroduced to the training chamber for 5 min. For the 24 hr cue test, mice were introduced to a novel context and allowed to habituation for 2 min before a 3 min, 80 dB white noise (CS) was presented. The percentage of freezing was calculated over the 3 min presentation period, unless otherwise noted.

Experimental Manipulations

SAHA Administration—SAHA (vorinostat, Zolinza) was purchased from TCI America, dissolved in vehicle (10% DMSO in saline), and administered at 25 mg/kg once per day i.p. for 10 days before behavioral assessment or tissue extraction. On the day of behavioral assessment, SAHA was injected 2 hr before entering the open field or threat recognition paradigms.

SAHA-Mediated Remote Memory Retrieval—*Tcf4*(+/−) mice and WT controls were trained and tested for 24 hr trace threat recognition before each genotype was split into two parametrically similar groups receiving either SAHA or vehicle for 10 days, beginning 24 hr after the first cue test. Then, 11 days after the initial training, mice were submitted to a second cue test.

HDAC2-ASO Identification and Administration—HDAC2-ASO (5′-CToCoAoCTTTTCGAGGTToCoCTA-3′) and control-ASO that targets no mouse or human genes (5′-GToToToTCAAATACACCToToCAT-3′) were generated by ISIS Pharmaceuticals using the phosphorothioate and 2′-MOE modified ASO platform. C, T, A, and G indicate 5-methylcytosine, thymine, adenine, and guanine nucleosides, respectively. Underlined residues are deoxynucleosides; all others are 2′-MOE nucleosides. All linkages are phosphorothioate except those indicate by “o” between residues, which are phosphodiester. Briefly, approximately 500 ASOs were designed against the full rat HDAC2 gene, with a higher density of ASOs targeting exonic regions. ASOs were electroporated into L2-RYC cells at a concentration of 5 mM, and RNA was extracted 24 hr after treatment for quantification. The most active ASOs were taken into a four-point dose response in L2-RYC cells, and five of the most potent ASOs that were complementary to mouse HDAC2 were injected by ICV bolus into C57BL/6 mice at a dose of 300 μg (n = 4). Two weeks after dosing, RNA was extracted from cortex, hippocampus, and spinal cord, and HDAC2 RNA reduction was measured by qPCR. The most active ASO (ASO1) was injected into C57BL/6 mice (700 μg ICV, n = 4), which were followed for 8 weeks post-treatment. At 8 weeks, mice were sacrificed and HDAC2 RNA was measured. For ICV injections, mice were anaesthetized with 2% isoflurane and secured in a stereotaxic frame (David Kopf Instruments). ASOs were diluted to 60 μg/μl in saline and injected 15 mg/kg ICV into the lateral ventricle (anterior/posterior [A/P], −0.2; medial/lateral [M/L], −1.0; dorsal/ventral [D/V], −2.4 to the bregma) of 2-month-old mice at a rate of 1 μl/min. After the injection, the needle was kept in place for 5 min before its removal, followed by suturing of the incision.

Gene Expression Analysis

For RNA sequencing, the hippocampus was extracted from 2-month-old mice (four animals per genotype) and the CA1 region was subdissected. Total mRNA was extracted (RNeasy,

QIAGEN), quality controlled (Bioanalyzer, Agilent), and poly(A) selected and sequenced (HudsonAlpha) on the Illumina platform (HiSeq v.4, paired end, 50 bp, 50 million reads). Reads were filtered by quality (90% of all bases were required to have a quality score > 20) and mapped using Tophat (maximum realign edit distance = 1,000, maximum edit distance = 2, maximum mismatches = 2, anchor length = 8, minimum intron length = 70, maximum intron length = 500,000) to the mm10 genome. Gene expression (fragments per kilobase per million [FPKM]) was calculated using Cufflinks, and DEGs were called by Cuffdiff, performing quartile normalization and using per-condition variances at a FDR < 0.05, and annotated with the NCBI refseq database. KEGG pathway and phenotypic analysis were performed using the free online WebGestalt software (http://bioinfo.vanderbilt.edu/webgestalt/). The Interactome network was derived from the original Tcf4(+/−), Tcf4(+/−) naive vehicle, and Tcf4(+/−) trained vehicle DEGs compared to WT controls using the free online NetworkAnalyst software (http://www.networkanalyst.ca/).

qRT-PCR was performed using standard procedures with exon-specific primers. Total mRNA was reverse transcribed using the iScript cDNA Synthesis Kit (Bio-Rad). qPCR was performed with the CFX96 Optical Reaction Module system (Bio-Rad) using SYBR green (Bio-Rad) with the following primers. Relative gene expression was determined using the comparative computed tomography method (Livak and Schmittgen, 2001) and normalized to Gapdh levels. *Hdac1* (Mm02391771_g1), *Hdac2* (Mm00515108_m1), *Grin2a* (Mm00433802_m1), *Grin2b* (Mm00433820_m1), *Arc* (Mm01204954_g1), and *Kl* (Mm00502002_m1) expression was detected using TaqMan Gene Expression Assays (Life Technologies) and normalized to the expression levels of *Gapdh* (Mm99999915_g1).

CpG Methylomics Analysis

For CpG dimethylation sequencing (MBD-seq), the hippocampus was extracted from 2-month-old mice (three animals per genotype) and the CA1 region was subdissected. Double-stranded DNA was extracted (DNeasy, QIAGEN) and sonicated to an average length of 300 bp as determined by gel electrophoreses. Methylated DNA fragments were then sequestered using the MethylMiner Methylated DNA Enrichment Kit (Life Technologies). The methylated DNA was then sized selected between 200 and 400 bp, amplified by PCR, and sequenced (HudsonAlpha) on the Illumina platform (HiSeq v.4, single end, 50 bp, 25 million reads).

Reads were trimmed (2 nt from the 5′ end), and PCR duplicates were removed (10.7 million to 22.6 million novel reads per sample) and mapped with Bowtie for Illumina to the mm10 genome. DMRs were then called using the published MEDIPS package and the R statistical programming language (window size [ws] = 300, extend = 300, shift = 0, uniq = T, quantile normalized, FDR = 0.1) (Lienhard et al., 2014).

Bisulfite Sequencing

Genomic DNA was extracted (DNeasy Blood and Tissue Kit, QIAGEN), treated with RNase A, and quantified (Quant-iT dsDNA HS Kit, Invitrogen) using the manufacturer's recommended protocols. Then, 450 ng of DNA per sample underwent bisulfite conversion (EZ DNA Methylation Kit, ZymoGenetics) and PCR amplification using bisulfite-

compatible primer sets targeting the following three loci: chromosome (chr) 5, 131,050,501–131,050,800; chr4, 155,716,201–155,716,500; and chr8, 29,059,501–29,059,801. PCR products were cloned using the TOPO-TA cloning system (Invitrogen) and transformed into Stbl3s (Invitrogen). Individual colonies were sequenced using Sanger sequencing (UAB Heflin Genomics Core). For each group, 20 individual clones were sequenced.

Cell Culture

Cultures were prepared from embryonic day 16 mouse hippocampal tissue. Briefly, 12-well tissue culture plates (Corning Life Sciences) were coated overnight at 37°C with poly-L-lysine (50 μg/ml) (Sigma-Aldrich) and rinsed two times with diH_2O. Hippocampal tissue was dissected in Hank's balanced salt solution (Life Technologies), digested in papain (Worthington Biochemical), and dissociated with fire-polished glass pipettes in Neurobasal medium (Life Technologies) supplemented with L-glutamine and B-27 (Life Technologies). The cell suspension was filtered through a 70-μm cell strainer and centrifuged. Cells were resuspended in the supplemented Neurobasal medium at a concentration of 125,000 cells/ml and plated. Cells were grown in a humidified CO_2 (5%) incubator at 37°C. Half of the medium was changed at 2 days in vitro (DIV) and every 4 days thereafter. RNA and protein were collected at 19 DIV following drug treatments. Treatments of hippocampal cultures were done at the following final drug concentrations: 10 μM control ASO and 10 μM HDAC2 ASOs. ASOs were added at 2 DIV and after every media change. Cells were harvested at 21 DIV.

Antibodies

Anti-histone H3 antibody (#3638, Cell Signaling Technology), anti-acetyl-histone H3 antibody (06-599, Millipore), anti-acetyl-histone H4 (Lys12) antibody (04-119, Millipore), and anti-actin antibody (ab3280, Abcam) were used.

E-Box Motif Analysis

Genes containing putative *Tcf4* binding sites surrounding their TSSs were identified using MotifMap (Daily et al., 2011). E-box sequences (5′-NCASCTGBYNYNKN-3′, 5′-CABCTGBY-3′, and 5′-RRCAGGTGBHV-3′) were identified at FDR < 0.05, normalized log odds > 0.65, and within 3 kb of annotated TSSs. A full list of genes can be found in Supplemental Information.

H3K9,14 and H4K12 ChIP-Seq Data Analysis

Using publically available data (GEO: GSE44868), differential histone acetylation levels of TSA-treated versus vehicle-treated mouse hippocampal tissue were assessed by mapping Fastq files generated from H3K9,14Ac and H4K12Ac chromatin immunoprecipitation sequencing (ChIP-seq) with Bowtie for Illumina to the mm10 genome. *Tcf4* locus acetylation patterns were generated by plotting differential wiggle plots (reads per kilobase per million [RPKM], 300 nt windows) of the TSA-treated samples versus the vehicle-treated samples. TSS acetylation levels were determined by quantifying read densities (RPKM) ±3 kb around TSSs.

Chemoinformatics

The *Tcf4* homology model was generated and rendered from the crystal structure of *Tcf3* as previously described (Sepp et al., 2012) using the Molecular Operating Environment by Chemical Computing Group.

LTP

Electrophysiology on Shaffer collaterals in the CA1 area was performed as previously described (Feng et al., 2010). Field excitatory post-synaptic potential (fEPSP) slopes over various stimulus intensities (1–30 mV) were used to assess baseline synaptic transmission. Subsequent stimuli were set to an intensity that evoked a fEPSP that had a slope of 50% or 25% of the maximum fEPSP slope. LTP was induced by theta burst stimulation. Synaptic efficacy was assessed for 3 hr following stimulation by recording fEPSPs every 20 s, and traces were averaged for every 2 min interval.

Statistics

Statistical analyses were performed with two-way ANOVA, followed by Tukey's post hoc analyses, or unpaired Student's t test using GraphPad Prism v.6. Cumulative distributions were evaluated using a Kolmogorov-Smirnov test. All data are represented as mean ± SEM. Statistical significance was set at $p < 0.05$, with a FDR < 0.05 for Cuffdiff and FDR < 0.1 for edgeR.

Supplementary Material

Refer to Web version on PubMed Central for supplementary material.

Acknowledgments

These studies were supported by grants from the Defense Advanced Research Projects Agency (HR0011-14-1-0001, HR0011-12-1-0015, and FA8650-13-C-7340 to J.D.S.), the NIH (MH57014, MH104158, and NR012688), the Civitan International, the Simons Foundation SFARI program, the McKnight Brain Research Foundation, and the Pitt-Hopkins Research Foundation. Special thanks are also due to Dr. Timothy Broderick for his intellectual support throughout the design and implementation of these experiments. The views, opinions, and findings contained in this article are those of the authors and should not be interpreted as representing the official views or policies of the Department of Defense or the U.S. Government. The authors in particular wish to thank the families and supporters of the Pitt-Hopkins Research Foundation for crucial financial and moral support at the earliest stages of initiating these studies. This work is dedicated to the memory of Kindal Kivisto.

References

Aberg KAK, McClay JLJ, Nerella S, Xie LYL, Clark SLS, Hudson ADA, Bukszár J, Adkins D, Hultman CM, Sullivan PF, et al. MBD-seq as a cost-effective approach for methylome-wide association studies: demonstration in 1500 case-control samples. Epigenomics. 2012; 4:605–621. [PubMed: 23244307]

Abraham WC. Metaplasticity: tuning synapses and networks for plasticity. Nat Rev Neurosci. 2008; 9:387. [PubMed: 18401345]

Bayly R, Chuen L, Currie RA, Hyndman BD, Casselman R, Blobel GA, LeBrun DP. E2A-PBX1 interacts directly with the KIX domain of CBP/p300 in the induction of proliferation in primary hematopoietic cells. J Biol Chem. 2004; 279:55362–55371. [PubMed: 15507449]

Blake DJ, Forrest M, Chapman RM, Tinsley CL, O'Donovan MC, Owen MJ. TCF4, schizophrenia, and Pitt-Hopkins syndrome. Schizophr Bull. 2010; 36:443–447. [PubMed: 20421335]

Breuer K, Foroushani AK, Laird MR, Chen C, Sribnaia A, Lo R, Winsor GL, Hancock REW, Brinkman FSL, Lynn DJ. InnateDB: systems biology of innate immunity and beyond—recent updates and continuing curation. Nucleic Acids Res. 2013; 41:D1228–D1233. [PubMed: 23180781]

Countryman RA, Kaban NL, Colombo PJ. Hippocampal c-fos is necessary for long-term memory of a socially transmitted food preference. Neurobiol Learn Mem. 2005; 84:175–183. [PubMed: 16122949]

Crawley JN. Designing mouse behavioral tasks relevant to autistic-like behaviors. Ment Retard Dev Disabil Res Rev. 2004; 10:248–258. [PubMed: 15666335]

Crawley JN. Translational animal models of autism and neurodevelopmental disorders. Dialogues Clin Neurosci. 2012; 14:293–305. [PubMed: 23226954]

Daily K, Patel VR, Rigor P, Xie X, Baldi P. MotifMap: integrative genome-wide maps of regulatory motif sites for model species. BMC Bioinformatics. 2011; 12:495. [PubMed: 22208852]

Day JJ, Kennedy AJ, Sweatt JD. DNA methylation and its implications and accessibility for neuropsychiatric therapeutics. Annu Rev Pharmacol Toxicol. 2015; 55:591–611. [PubMed: 25340930]

de Pontual L, Mathieu Y, Golzio C, Rio M, Malan V, Boddaert N, Soufflet C, Picard C, Durandy A, Dobbie A, et al. Mutational, functional, and expression studies of the TCF4 gene in Pitt-Hopkins syndrome. Hum Mutat. 2009; 30:669–676. [PubMed: 19235238]

Dubal DB, Yokoyama JS, Zhu L, Broestl L, Worden K, Wang D, Sturm VE, Kim D, Klein E, Yu GQ, et al. Life extension factor klotho enhances cognition. Cell Rep. 2014; 7:1065–1076. [PubMed: 24813892]

Feng J, Zhou Y, Campbell SL, Le T, Li E, Sweatt JD, Silva AJ, Fan G. Dnmt1 and Dnmt3a maintain DNA methylation and regulate synaptic function in adult forebrain neurons. Nat Neurosci. 2010; 13:423–430. [PubMed: 20228804]

Fields RD. Myelination: an overlooked mechanism of synaptic plasticity? Neuroscientist. 2005; 11:528–531. [PubMed: 16282593]

Fischer A, Sananbenesi F, Wang X, Dobbin M, Tsai LH. Recovery of learning and memory is associated with chromatin remodelling. Nature. 2007; 447:178–182. [PubMed: 17468743]

Forrest MP, Hill MJ, Quantock AJ, Martin-Rendon E, Blake DJ. The emerging roles of TCF4 in disease and development. Trends Mol Med. 2014; 20:322–331. [PubMed: 24594265]

Fujita E, Tanabe Y, Shiota A, Ueda M, Suwa K, Momoi MY, Momoi T. Ultrasonic vocalization impairment of Foxp2 (R552H) knockin mice related to speech-language disorder and abnormality of Purkinje cells. Proc Natl Acad Sci USA. 2008; 105:3117–3122. [PubMed: 18287060]

Ghosh PS, Friedman NR, Ghosh D. Pitt-Hopkins syndrome in a boy with Charcot Marie Tooth disease type 1A: a rare co-occurrence of 2 genetic disorders. J Child Neurol. 2012; 27:1602–1606. [PubMed: 22378661]

Gräff J, Tsai LH. The potential of HDAC inhibitors as cognitive enhancers. Annu Rev Pharmacol Toxicol. 2013; 53:311–330. [PubMed: 23294310]

Gräff J, Kim D, Dobbin MM, Tsai LH. Epigenetic regulation of gene expression in physiological and pathological brain processes. Physiol Rev. 2011; 91:603–649. [PubMed: 21527733]

Gräff J, Joseph NF, Horn ME, Samiei A, Meng J, Seo J, Rei D, Bero AW, Phan TX, Wagner F, et al. Epigenetic priming of memory updating during reconsolidation to attenuate remote fear memories. Cell. 2014; 156:261–276. [PubMed: 24439381]

Grubišić V, Kennedy AJ, Sweatt JD, Parpura V. Pitt-Hopkins mouse model has altered particular gastrointestinal transits in vivo. Autism Res. 2015; 8:629–633. [PubMed: 25728630]

Gu Y, McIlwain KL, Weeber EJ, Yamagata T, Xu B, Antalffy BA, Reyes C, Yuva-Paylor L, Armstrong D, Zoghbi H, et al. Impaired conditioned fear and enhanced long-term potentiation in Fmr2 knock-out mice. J Neurosci. 2002; 22:2753–2763. [PubMed: 11923441]

Guan JS, Haggarty SJ, Giacometti E, Dannenberg JH, Joseph N, Gao J, Nieland TJ, Zhou Y, Wang X, Mazitschek R, et al. HDAC2 negatively regulates memory formation and synaptic plasticity. Nature. 2009; 459:55–60. [PubMed: 19424149]

Haettig J, Stefanko DP, Multani ML, Figueroa DX, McQuown SC, Wood MA. HDAC inhibition modulates hippocampus-dependent long-term memory for object location in a CBP-dependent manner. Learn Mem. 2011; 18:71–79. [PubMed: 21224411]

Hamers FP, Koopmans GC, Joosten EA. CatWalk-assisted gait analysis in the assessment of spinal cord injury. J Neurotrauma. 2006; 23:537–548. [PubMed: 16629635]

Hetze S, Römer C, Teufelhart C, Meisel A, Engel O. Gait analysis as a method for assessing neurological outcome in a mouse model of stroke. J Neurosci Methods. 2012; 206:7–14. [PubMed: 22343052]

Huang Y, Chavez L, Chang X, Wang X, Pastor WA, Kang J, Zepeda-Martínez JA, Pape UJ, Jacobsen SE, Peters B, Rao A. Distinct roles of the methylcytosine oxidases Tet1 and Tet2 in mouse embryonic stem cells. Proc Natl Acad Sci USA. 2014; 111:1361–1366. [PubMed: 24474761]

Jones PA. Functions of DNA methylation: islands, start sites, gene bodies and beyond. Nat Rev Genet. 2012; 13:484–492. [PubMed: 22641018]

Kaas GA, Zhong C, Eason DE, Ross DL, Vachhani RV, Ming GL, King JR, Song H, Sweatt JD. TET1 controls CNS 5-methylcytosine hydroxylation, active DNA demethylation, gene transcription, and memory formation. Neuron. 2013; 79:1086–1093. [PubMed: 24050399]

Kennedy AJ, Sweatt JD. Drugging the methylome: DNA methylation and memory. Crit Rev Biochem Mol Biol. 2016; 51:185–194. [PubMed: 26915423]

Kilgore M, Miller CA, Fass DM, Hennig KM, Haggarty SJ, Sweatt JD, Rumbaugh G. Inhibitors of class 1 histone deacetylases reverse contextual memory deficits in a mouse model of Alzheimer's disease. Neuropsychopharmacology. 2010; 35:870–880. [PubMed: 20010553]

Kordasiewicz HB, Stanek LM, Wancewicz EV, Mazur C, McAlonis MM, Pytel KA, Artates JW, Weiss A, Cheng SH, Shihabuddin LS, et al. Sustained therapeutic reversal of Huntington's disease by transient repression of huntingtin synthesis. Neuron. 2012; 74:1031–1044. [PubMed: 22726834]

Lee PR, Fields RD. Regulation of myelin genes implicated in psychiatric disorders by functional activity in axons. Front Neuroanat. 2009; 3:4. [PubMed: 19521541]

Lennertz L, Rujescu D, Wagner M, Frommann I, Schulze-Rauschenbach S, Schuhmacher A, Landsberg MW, Franke P, Möller HJ, Wölwer W, et al. Novel schizophrenia risk gene TCF4 influences verbal learning and memory functioning in schizophrenia patients. Neuropsychobiology. 2011; 63:131–136. [PubMed: 21228604]

Lienhard M, Grimm C, Morkel M, Herwig R, Chavez L. MEDIPS: genome-wide differential coverage analysis of sequencing data derived from DNA enrichment experiments. Bioinformatics. 2014; 30:284–286. [PubMed: 24227674]

Liu L, Wong TP, Pozza MF, Lingenhoehl K, Wang Y, Sheng M, Auberson YP, Wang YT. Role of NMDA receptor subtypes in governing the direction of hippocampal synaptic plasticity. Science. 2004; 304:1021–1024. [PubMed: 15143284]

Livak KJ, Schmittgen TD. Analysis of relative gene expression data using real-time quantitative PCR and the 2(−Delta Delta C(T)) method. Methods. 2001; 25:402–408. [PubMed: 11846609]

Lopez-Atalaya JP, Ito S, Valor LM, Benito E, Barco A. Genomic targets, and histone acetylation and gene expression profiling of neural HDAC inhibition. Nucleic Acids Res. 2013; 41:8072–8084. [PubMed: 23821663]

Maini I, Cantalupo G, Turco EC, De Paolis F, Magnani C, Parrino L, Terzano MG, Pisani F. Clinical and polygraphic improvement of breathing abnormalities after valproate in a case of Pitt-Hopkins syndrome. J Child Neurol. 2012; 27:1585–1588. [PubMed: 22378662]

Massari ME, Grant PA, Pray-Grant MG, Berger SL, Workman JL, Murre C. A conserved motif present in a class of helix-loop-helix proteins activates transcription by direct recruitment of the SAGA complex. Mol Cell. 1999; 4:63–73. [PubMed: 10445028]

Meng L, Ward AJ, Chun S, Bennett CF, Beaudet AL, Rigo F. Towards a therapy for Angelman syndrome by targeting a long non-coding RNA. Nature. 2015; 518:409–412. [PubMed: 25470045]

Miller CA, Campbell SL, Sweatt JD. DNA methylation and histone acetylation work in concert to regulate memory formation and synaptic plasticity. Neurobiol Learn Mem. 2008; 89:599–603. [PubMed: 17881251]

Peippo M, Ignatius J. Pitt-Hopkins syndrome. Mol Syndromol. 2012; 2:171–180. [PubMed: 22670138]

Quednow BB, Ettinger U, Mössner R, Rujescu D, Giegling I, Collier DA, Schmechtig A, Kühn KU, Möller HJ, Maier W, et al. The schizophrenia risk allele C of the TCF4 rs9960767 polymorphism

disrupts sensorimotor gating in schizophrenia spectrum and healthy volunteers. J Neurosci. 2011; 31:6684–6691. [PubMed: 21543597]

Quinn JJ, Loya F, Ma QD, Fanselow MS. Dorsal hippocampus NMDA receptors differentially mediate trace and contextual fear conditioning. Hippocampus. 2005; 15:665–674. [PubMed: 15959918]

Rannals MD, Hamersky GR, Page SC, Campbell MN, Briley A, Gallo RA, Phan BN, Hyde TM, Kleinman JE, Shin JH, et al. Psychiatric risk gene transcription factor 4 regulates intrinsic excitability of prefrontal neurons via repression of SCN10a and KCNQ1. Neuron. 2016; 90:43–55. [PubMed: 26971948]

Roullet FI, Crawley JN. Mouse models of autism: testing hypotheses about molecular mechanisms. Curr Top Behav Neurosci. 2011; 7:187–212. [PubMed: 21225409]

Sepp M, Pruunsild P, Timmusk T. Pitt-Hopkins syndrome-associated mutations in TCF4 lead to variable impairment of the transcription factor function ranging from hypomorphic to dominant-negative effects. Hum Mol Genet. 2012; 21:2873–2888. [PubMed: 22460224]

Shepherd JD, Bear MF. New views of Arc, a master regulator of synaptic plasticity. Nat Neurosci. 2011; 14:279–284. [PubMed: 21278731]

Shepherd JD, Rumbaugh G, Wu J, Chowdhury S, Plath N, Kuhl D, Huganir RL, Worley PF. Arc/Arg3.1 mediates homeostatic synaptic scaling of AMPA receptors. Neuron. 2006; 52:475–484. [PubMed: 17088213]

Shin J, Ming GL, Song H. DNA modifications in the mammalian brain. Philos Trans R Soc Lond B Biol Sci. 2014; 369:1–10.

Shu W, Cho JY, Jiang Y, Zhang M, Weisz D, Elder GA, Schmeidler J, De Gasperi R, Sosa MAG, Rabidou D, et al. Altered ultrasonic vocalization in mice with a disruption in the Foxp2 gene. Proc Natl Acad Sci USA. 2005; 102:9643–9648. [PubMed: 15983371]

Sweatt JD. Pitt-Hopkins syndrome: intellectual disability due to loss of TCF4-regulated gene transcription. Exp Mol Med. 2013; 45:e21. [PubMed: 23640545]

Tan CP, Nakielny S. Control of the DNA methylation system component MBD2 by protein arginine methylation. Mol Cell Biol. 2006; 26:7224–7235. [PubMed: 16980624]

Tsankova N, Renthal W, Kumar A, Nestler EJ. Epigenetic regulation in psychiatric disorders. Nat Rev Neurosci. 2007; 8:355–367. [PubMed: 17453016]

Wu H, Lima WF, Zhang H, Fan A, Sun H, Crooke ST. Determination of the role of the human RNase H1 in the pharmacology of DNA-like antisense drugs. J Biol Chem. 2004; 279:17181–17189. [PubMed: 14960586]

Yashiro K, Philpot BD. Regulation of NMDA receptor subunit expression and its implications for LTD, LTP, and metaplasticity. Neuropharmacology. 2008; 55:1081–1094. [PubMed: 18755202]

Zhang J, Kalkum M, Yamamura S, Chait BT, Roeder RG. E protein silencing by the leukemogenic AML1-ETO fusion protein. Science. 2004; 305:1286–1289. [PubMed: 15333839]

Zhuang Y, Cheng P, Weintraub H. B-lymphocyte development is regulated by the combined dosage of three basic helix-loop-helix genes, E2A, E2-2, and HEB. Mol Cell Biol. 1996; 16:2898–2905. [PubMed: 8649400]

Zweier C, Sticht H, Bijlsma EK, Clayton-Smith J, Boonen SE, Fryer A, Greally MT, Hoffmann L, den Hollander NS, Jongmans M, et al. Further delineation of Pitt-Hopkins syndrome: phenotypic and genotypic description of 16 novel patients. J Med Genet. 2008; 45:738–744. [PubMed: 18728071]

Highlights

- A *Tcf4*(+/−) mouse model is reported for Pitt-Hopkins syndrome (PTHS)
- HDAC inhibition rescues learning and memory deficits of PTHS mice
- Hdac2 is a therapeutic target for cognitive enhancement
- Genes with altered mRNA and CpG Me due to learning are dysregulated in PTHS

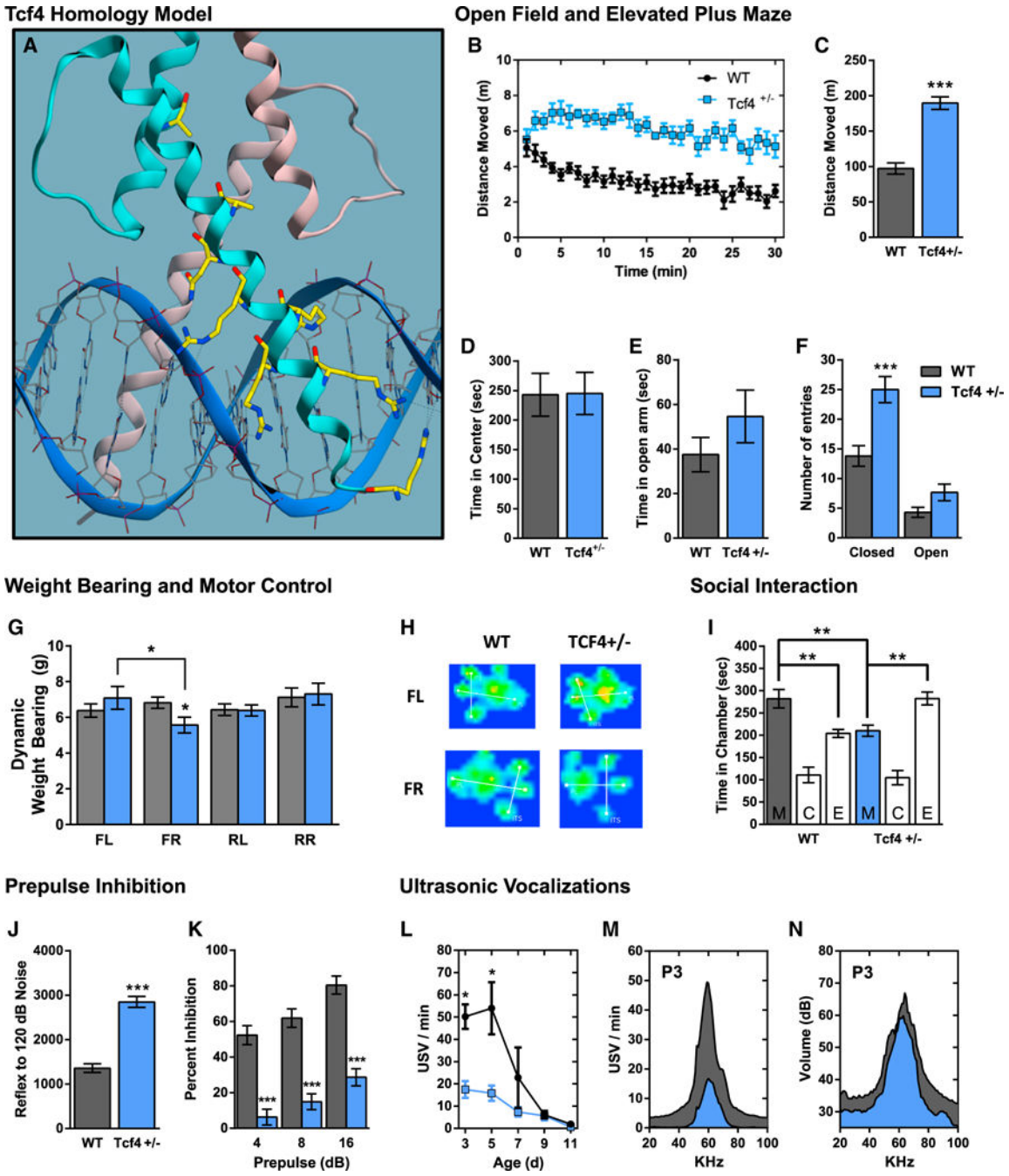

Figure 1. *Tcf4*(+/−) Mice Are Hyperactive, Display Motor Incoordination, Have Reduced Prepulse Inhibition, and Show Autistic-like Behavior

(A) Homology model of Tcf4 protein (teal) with NeuroD2 (tan) bound to DNA. Mutations in Tcf4 protein that cause PTHS (yellow) are predominately basic residues necessary for DNA backbone association.

(B and C) Open field. Distance traveled per minute during a 30 m trial. *Tcf4*(+/−) mice show hyperactivity and a reduced ability to habituate to an open field.

(D) Thigmotaxis, a behavior associated with anxiety, during the open field task.

(E and F) Elevated plus maze. Arm entries during a 5 m trial. *Tcf4*(+/−) mice cross more frequently between arms but do not elicit significantly altered anxiety toward open arms.
(G) Dynamic weight bearing. *Tcf4*(+/−) mice place more body weight on the front left paw than on the front right.
(H) Representative images of *Tcf4*(+/−) mice placing more pressure on the front left paw than on the front right while ambulating across a catwalk.
(I) Three-chamber social interaction task. Mice are placed into the center (C) of a three-chamber apparatus, where the distal chambers contained either an empty cylindrical cage (E) or a cylindrical cage holding a novel mouse (M) of equivalent age, gender, and strain. *Tcf4*(+/−) mice show social aversion, preferring the chamber with an empty cage to that with the novel mouse.
(J) Start reflex. *Tcf4*(+/−) mice have an enhance startle reflex to unexpected 120 dB sound bursts.
(K) *Tcf4*(+/−) mice have deficits in prepulse inhibition of the startle reflex when the 120 dB sound burst is preempted by 69, 73, and 81 dB pulses over 65 dB background white noise.
(L) USVs in *Tcf4*(+/−) pups P3 and P5 were significantly infrequent when removed from the nest.
(M and N) Occurrence (M) and traces (N) across ultrasonic frequencies elicited by P3 pups. All data shown are means ± SEM from 12 mice per genotype at 2–3 months of age, with the exception of the USV experiments, which were performed with pups (P3–P11) and 6 mice per genotype. *$p < 0.05$, **$p < 0.01$, ***$p < 0.001$.

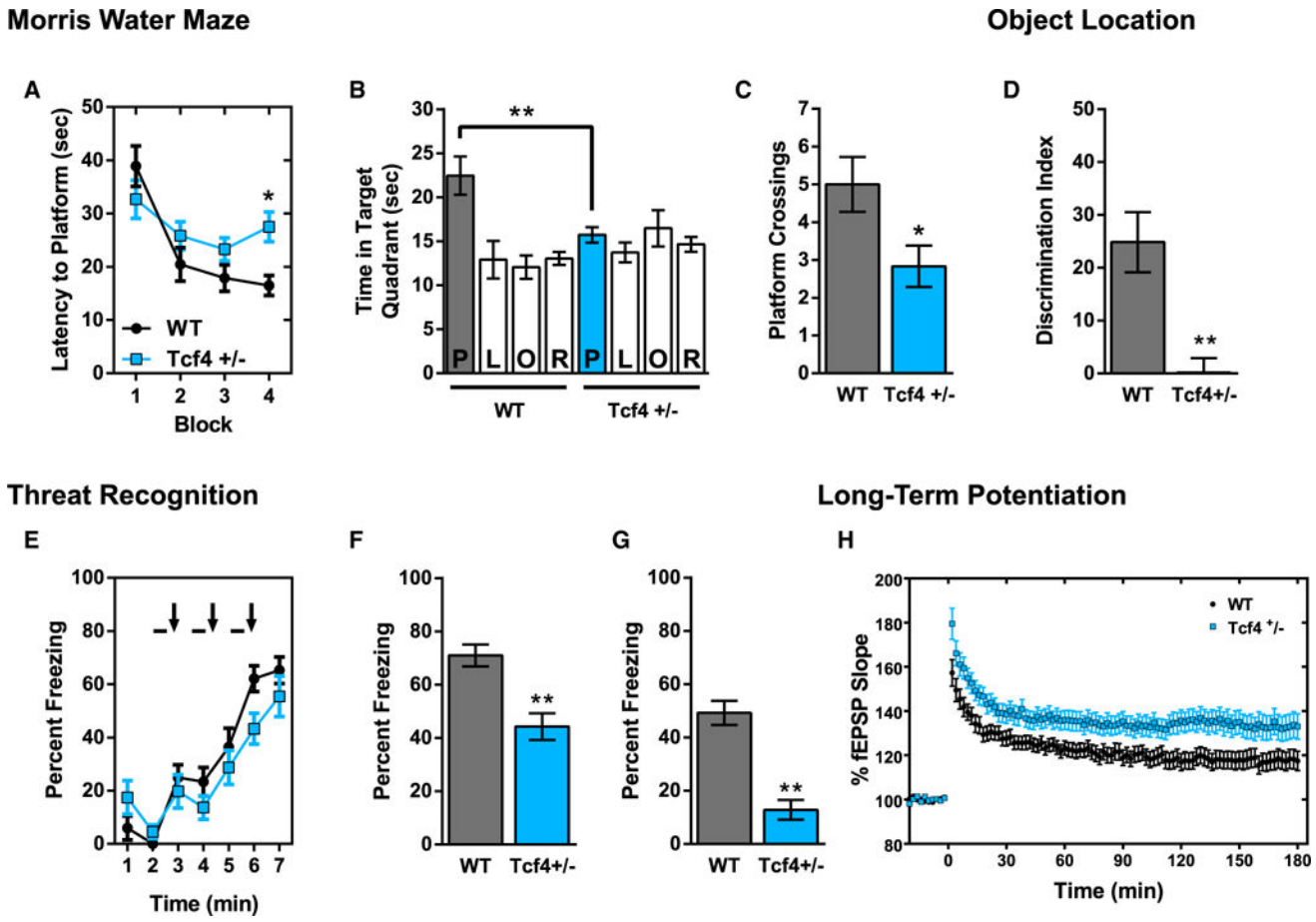

Figure 2. *Tcf4*(+/−) Mice Have Deficits in Associative and Spatial Learning and Memory, Prepulse Inhibition, and Enhanced LTP across Schaffer Collaterals

(A–C) MWM hidden platform task. *Tcf4*(+/−) mice show reduced spatial learning in locating the hidden platform.

(D) 24 hr OLM. Mice interacted for 10 min with 50 ml beakers, and 24 hr memory was tested by moving one beaker to a novel location and measuring the amount of time interacting with the novel location (t_N) versus the familiar location (t_F). Discrimination index = $(t_N - t_F)/(t_N \times t_F)$.

(E) Trace threat recognition training. Mice were presented with a 30 s white noise tone (CS, line), followed by a 15 s delay, and then a 1 s, 0.5 mA foot shock (US, arrow) three times over the course of a 7.5 m trial. *Tcf4*(+/−) mice do not show deficits in freezing during training.

(F) 24 hr contextual test. *Tcf4*(+/−) mice show reduced freezing during a 5 m test in the training context.

(G) 24 hr cued test. *Tcf4*(+/−) mice show reduced freezing when placed in a novel context and presented with a 3 m white noise tone.

(H) *Tcf4*(+/−) mice have enhanced LTP across Schaffer collaterals when activated with (1×) theta burst stimulation.

All data shown are means ± SEM from 6–12 mice per genotype at 2–3 months of age. LTP from 55–58 hippocampal slices per group. *$p < 0.05$, **$p < 0.01$, ***$p < 0.001$.

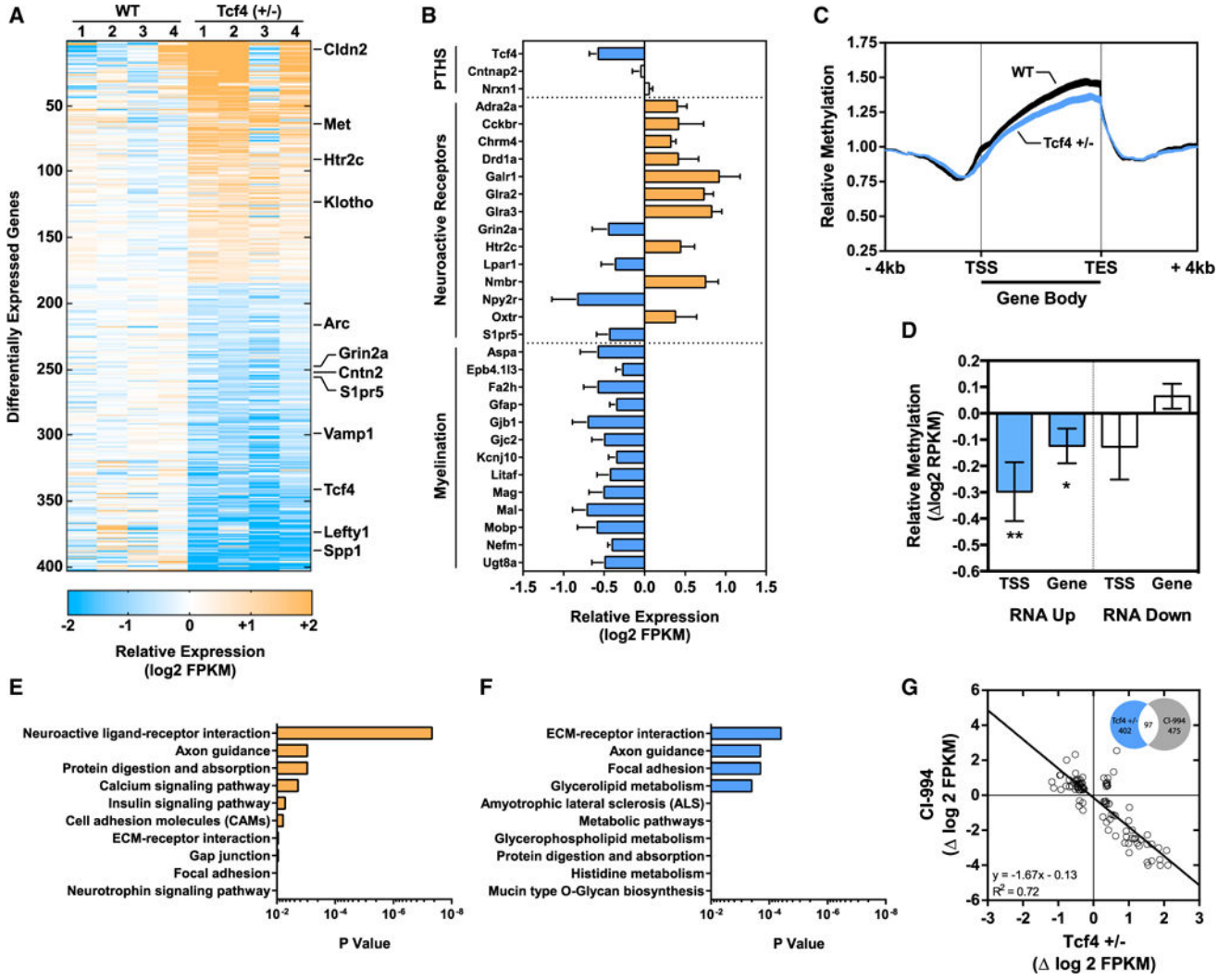

Figure 3. Gene Expression Patterns and Altered CpG Methylation Caused by *Tcf4*(+/−) in the Hippocampus

(A) Heatmap of poly(A) RNA-seq DEGs in the *Tcf4*(+/−) hippocampus showing individual replicates (FDR < 0.05).

(B) Gene expression grouped by their relation to PTHS, neuroactive receptors, and myelination (blue, downregulated; orange, upregulated; white, not significant).

(C) Relative global methylation across gene bodies. Curve thickness is ±SEM.

(D) DEG gene body and TSS methylation changes.

(E) Top ten represented upregulated KEGG pathways in *Tcf4*(+/−) mice as ranked by Benjamini and Hochberg (B–H) adjusted p value.

(F) Downregulated KEGG pathways in *Tcf4*(+/−) mice.

(G) In *Tcf4*(+/−) hippocampal tissue, 97 deregulated genes are affected by the administration of the class I Hdac inhibitor CI-994 and have a strong negative correlation ($R^2 = 0.72$).

All data shown are from four mice per genotype at 2 months of age.

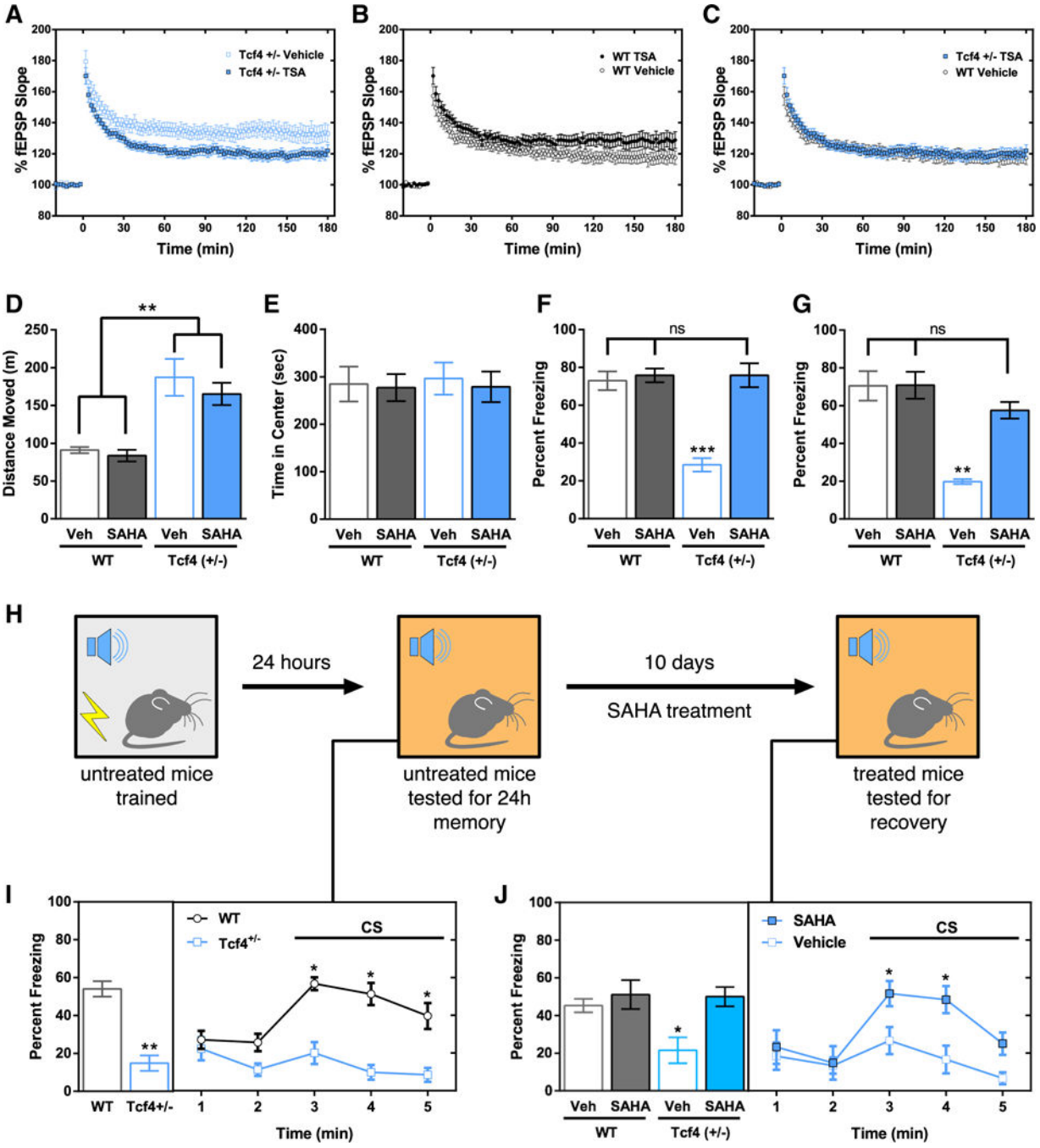

Figure 4. HDAC Inhibition Rescues LTP and Memory in *Tcf4*(+/−) Mice

(A) TSA reduces LTP in the CA1 area of *Tcf4*(+/−) mice.

(B) TSA enhances LTP in the CA1 area of WT controls.

(C) TSA normalizes LTP in *Tcf4*(+/−) mice relative to untreated WT controls.

(D and E) SAHA has no significant effect on *Tcf4*(+/−) hyperactivity or thigmotaxis in an open field.

(F and G) SAHA administered 25 mg/kg i.p. for 10 days rescues *Tcf4*(+/−) deficits in 24 hr contextual and trace-cued threat recognition memory.

(H) Schematic of the experimental paradigm to test SAHA-mediated memory retrieval post-training. *Tcf4*(+/−) mice were trained using the trace threat recognition protocol, tested for memory at 24 hr, and then treated with SAHA for 10 days before being test again for remote memory recall.

(I) *Tcf4*(+/−) mice have 24 hr memory deficits. Bars represent freezing during the first 2 minutes of the cue presentation.

(J) SAHA treatment after training improves remote memory recall in *Tcf4*(+/−) mice.

All data shown are means ± SEM from six mice per group at 2 months of age. *$p < 0.05$, **$p < 0.01$, ***$p < 0.001$.

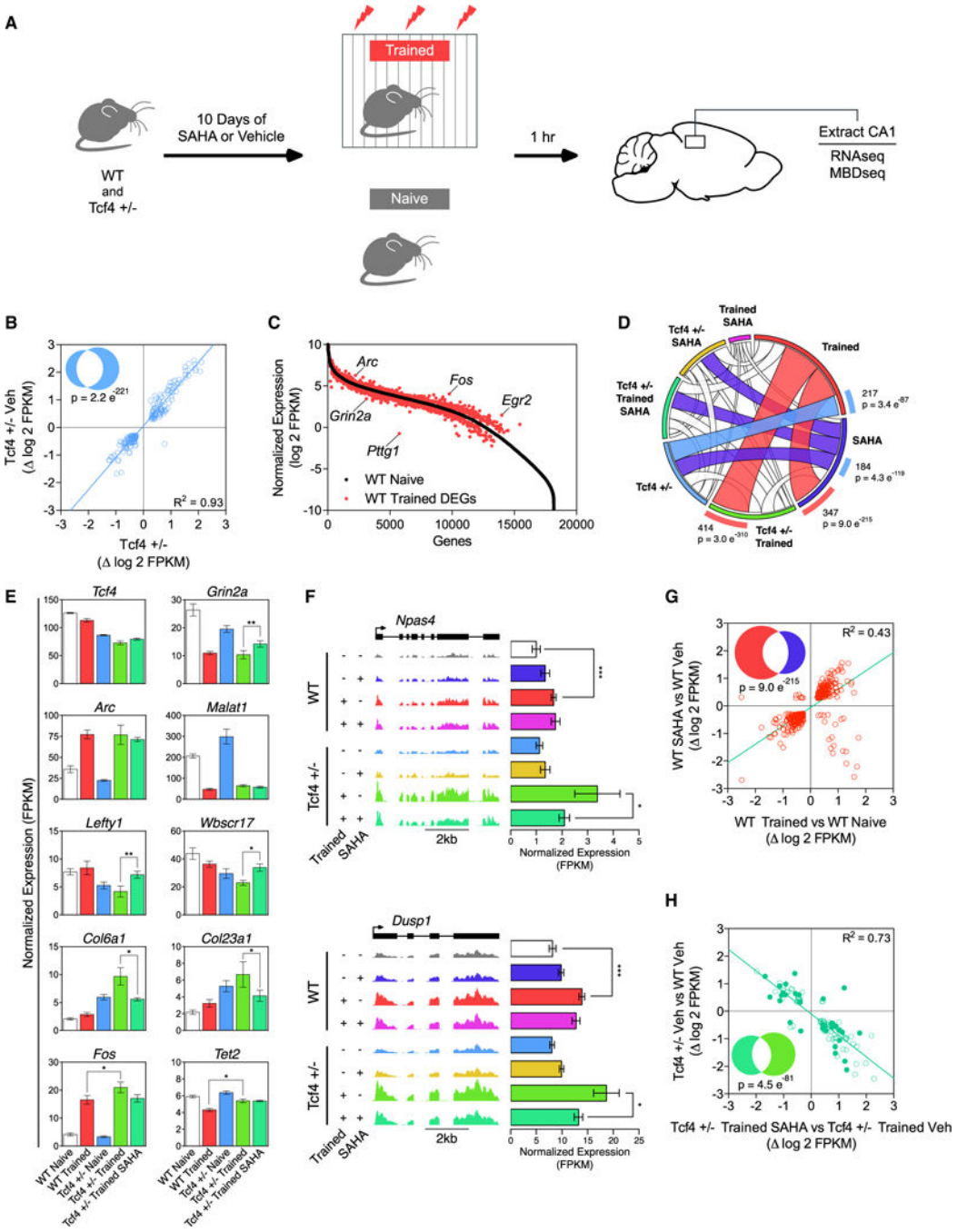

Figure 5. Effects of SAHA on *Tcf4*(+/−) and Memory-Associated Gene Expression

(A) *Tcf4*(+/−) and WT mice were treated with SAHA or vehicle control for 10 days and either kept naive or trained in threat recognition. RNA and methylated DNA were then isolated from the CA1 region of the hippocampus 1 hr after training.

(B) Correlation between the original *Tcf4*(+/−) RNA-seq and the *Tcf4*(+/−) naive vehicle group DEG lists relative to WT controls.

(C) Expression of all genes in the WT naive vehicle group, and significant changes in transcription associated with training.

(D) Chord diagram showing the number of overlapping DEGs between each of the seven most relevant pairwise comparisons among the eight datasets. The most significant overlaps in gene identity between comparisons are filled with color, and the significance of the overlap is listed on the perimeter.
(E) Expression profiles of *Tcf4*(+/−) DEGs for select datasets.
(F) RNA-seq read density and normalized expression for the dysregulated IEGs *Npas4* and *Dusp1*.
(G) SAHA elicits an expression profile similar to that of training in WT mice. Scatterplot of WT naive SAHA versus WT naive vehicle and WT trained vehicle versus WT naive vehicle. Only genes significant in both comparisons are shown.
(H) SAHA normalizes the expression of *Tcf4*(+/−) DEGs post-training. Scatterplot of Tcf4(+/−) naive vehicle versus WT naive vehicle and Tcf4(+/−) trained SAHA versus Tcf4(+/−) trained vehicle. Only genes significant in both comparisons are shown.
All data shown are means ± SEM from three mice per group at 2 months of age. *$p < 0.05$, **$p < 0.01$, ***$p < 0.001$.

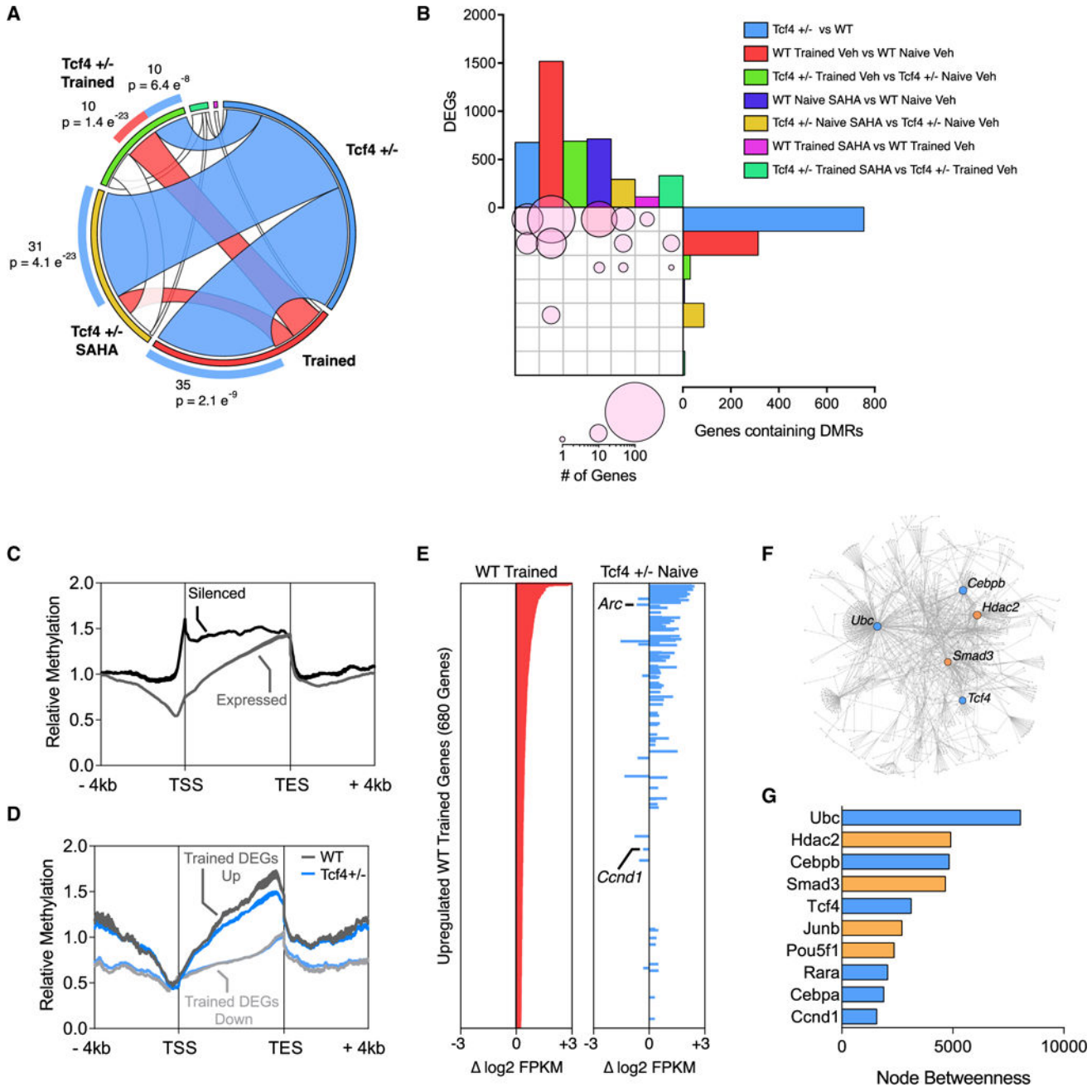

Figure 6. *Tcf4*(+/−) DMRs Are Associated with Trained DEGs

(A) Chord diagram showing the number of overlapping genes containing DMRs between each of the seven most relevant pairwise comparisons among the eight datasets. The most significant overlaps in gene identity between comparisons are filled with color, and the significance of the overlap is listed on the perimeter.

(B) Cross-comparison of DEGs and genes containing DMRs for each pairwise comparison, in which significant overlaps ($p < 0.05$) between datasets are shown as circles in the matrix.

(C) Differential CpG methylation profile of expressed and silenced genes in the hippocampus of WT mice. Curve thickness is ±SEM.

(D) Differential CpG methylation profile of genes upregulated and downregulated after training. Genes upregulated after training in WT mice are significantly hypomethylated in *Tcf4*(+/−) mice.

(E) Genes with significantly upregulated expression after training in WT mice have significantly increased baseline expression in *Tcf4*(+/−) naive mice compared to WT naive controls.

(F) Interactome network derived from the original *Tcf4*(+/−), *Tcf4*(+/−) naive vehicle, and *Tcf4*(+/−) trained vehicle DEGs, highlighting gene products with a high degree of interaction among these *Tcf4*(+/−) DEGs.

(G) *Ubc* and *Hdac2* are identified as the most interconnected gene products in the *Tcf4*(+/−) DEG datasets.

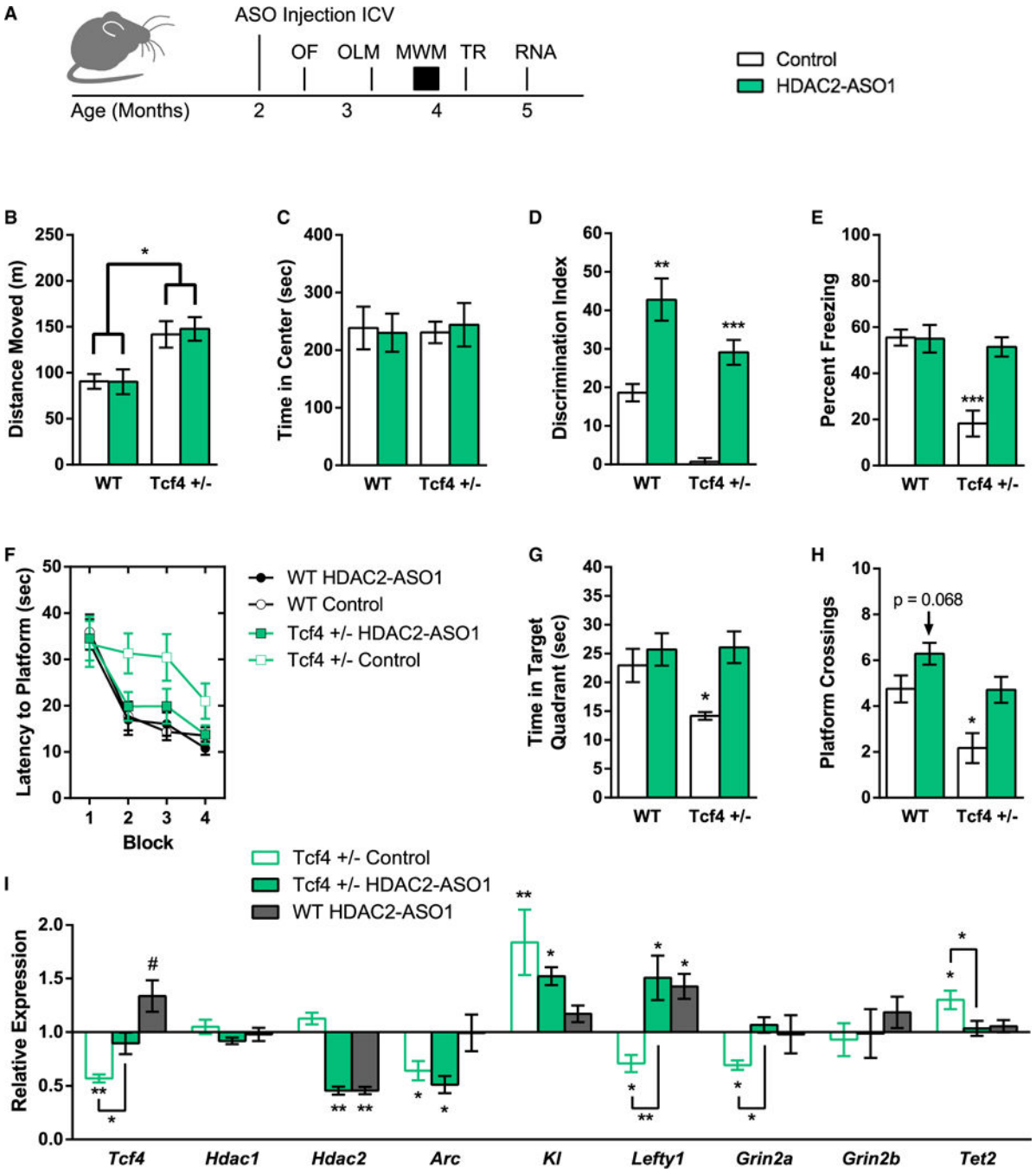

Figure 7. HDAC2 Knockdown Enhances *Tcf4* Expression and Rescues Spatial and Threat Recognition Memory in *Tcf4*(+/−) Mice

(A) Schematic of surgical, behavioral, and expression analysis. Mice were injection with HDAC2-ASO1 or control at 2 months of age followed by a behavioral battery including open field (OF), object location memory (OLM), Morris water maze (MWM), and contextual threat recognition (TR). At 5 months, RNA was extracted from the hippocampus for analysis.

(B and C) HDAC2-ASO1 has no significant effect on *Tcf4*(+/−) hyperactivity or thigmotaxis in an open field.

(D) HDAC2-ASO1 significantly improves 24 hr object location memory in *Tcf4*(+/−) and wild-type mice.
(E) HDAC2-ASO1 rescues 24 hr contextual threat recognition memory in *Tcf4*(+/−) treated mice.
(F–H) HDAC2-ASO1 rescues spatial memory in the MWM task by increasing the time spent in the target quadrant and the number of platform crossing in *Tcf4*(+/−) treated mice.
(I) PCR expression analysis. *HDAC2* knockdown 3 months after ICV injection boosts *Tcf4* transcription and normalizes the expression of *Lefty1*, *Grin2a*, and *Tet2*.
All data shown are means ± SEM from seven to ten mice per group at 2–5 months of age. #p = 0.052, *p < 0.05, **p < 0.01, ***p < 0.001.